



HAL
open science

Optimized precursor to simplify assignment transfer between backbone resonances and stereospecifically labelled valine and leucine methyl groups: application to human Hsp90 N-terminal domain

Faustine Henot, Rime Kerfah, Ricarda Törner, Pavel Macek, Elodie Crublet, Pierre Gans, Matthias Frech, Olivier Hamelin, Jérôme Boisbouvier

► To cite this version:

Faustine Henot, Rime Kerfah, Ricarda Törner, Pavel Macek, Elodie Crublet, et al.. Optimized precursor to simplify assignment transfer between backbone resonances and stereospecifically labelled valine and leucine methyl groups: application to human Hsp90 N-terminal domain. *Journal of Biomolecular NMR*, 2021, 75 (6-7), pp.221-232. 10.1007/s10858-021-00370-0 . hal-03262389

HAL Id: hal-03262389

<https://hal.science/hal-03262389>

Submitted on 17 Jun 2021

HAL is a multi-disciplinary open access archive for the deposit and dissemination of scientific research documents, whether they are published or not. The documents may come from teaching and research institutions in France or abroad, or from public or private research centers.

L'archive ouverte pluridisciplinaire **HAL**, est destinée au dépôt et à la diffusion de documents scientifiques de niveau recherche, publiés ou non, émanant des établissements d'enseignement et de recherche français ou étrangers, des laboratoires publics ou privés.

1 **Optimized Precursor to Simplify Assignment Transfer between Backbone**
2 **Resonances and Stereospecifically labelled Valine and Leucine Methyl**
3 **Groups: Application to Human Hsp90 N-Terminal Domain**

4
5
6 Faustine Henot¹, Rime Kerfah², Ricarda Törner¹, Pavel Macek^{1,2}, Elodie Crublet², Pierre
7 Gans¹, Matthias Frech³, Olivier Hamelin⁴, Jerome Boisbouvier¹. *

8
9
10 1. Univ. Grenoble Alpes, CNRS, CEA, Institut de Biologie Structurale (IBS),
11 71, avenue des martyrs, F-38044 Grenoble, France.

12 2. NMR-Bio, 5 place Robert Schuman, F-38025 Grenoble, France.

13 3. Discovery Technologies, Merck KGaA, Frankfurter Straße 250, 64293 Darmstadt, Germany.

14 4. Univ. Grenoble Alpes, CEA, CNRS, IRIG, CBM-F-38000 Grenoble. France.

15 * correspondence to be addressed to: jerome.boisbouvier@ibs.fr

16
17
18 **Abstract:**

19
20 Methyl moieties are highly valuable probes for quantitative NMR studies of large proteins.
21 Hence, their assignment is of the utmost interest to obtain information on both interactions and
22 dynamics of proteins in solution. Here, we present the synthesis of a new precursor that allows
23 connection of leucine and valine pro-*S* methyl moieties to backbone atoms by linear ¹³C-chains.
24 This optimized ²H/¹³C-labelled acetolactate precursor can be combined with existing ¹³C/²H-
25 alanine and isoleucine precursors in order to directly transfer backbone assignment to the
26 corresponding methyl groups. Using this simple approach leucine and valine pro-*S* methyl
27 groups can be assigned using a single sample without requiring correction of ¹H/²H isotopic
28 shifts on ¹³C resonances. The approach was demonstrated on the N-terminal domain of human
29 HSP90, for which complete assignment of Ala-β, Ile-δ₁, Leu-δ₂, Met-ε, Thr-γ and Val-γ₂ methyl
30 groups was obtained.

31
32
33
34
35
36
37
38
39
40 Keywords: NMR, assignment, methyl groups, acetolactate, HSP90

1 **Introduction:**

2
3 Solution state NMR is the method of choice to characterize proteins at atomic level and
4 to probe their dynamics over a wide range of biologically relevant timescales. However, for a
5 long-time, study of high molecular weight proteins by NMR remained a challenge, notably due
6 to the extensive line broadening of NMR signals in large proteins. Methyl groups have been
7 widely studied and are extremely useful to overcome this issue that has hampered, in the past,
8 quantitative NMR studies on large proteins. Indeed, due to the proton multiplicity and their
9 favorable relaxation properties, methyl groups allow the detection of NMR signals even for
10 large proteins (Tugarinov et al. 2003). Nowadays, methyl groups are important probes to
11 investigate molecular dynamics (Sprangers and Kay 2007) and to provide functional insight
12 (Rosenzweig et al. 2013; Mas et al. 2018) on assemblies weighing up to 1 MDa. Specific
13 labelling of methyl groups on perdeuterated large proteins allows the measurement of long-
14 range distance restraints, up to 12 Å. (Sounier et al. 2007; Ayala et al. 2020) and enables, in
15 combination with other structural biology techniques such as SANS/SAXS (Lapinaite et al.
16 2013) or Cryo-EM (Gauto et al. 2019), to solve the structure of complexes of several hundreds
17 of kDa.

18 For the past 20 years, a plethora of protocols overexpressing proteins in M9²H₂O based
19 *E.coli* growth medium and leading to specific protonation of methyl groups in perdeuterated
20 proteins without scrambling of protons to other sites have been elaborated. On one hand, the
21 direct incorporation of the methyl labelled amino acid in M9²H₂O is employed for the specific
22 labelling of ¹³C¹H₃-alanine (Isaacson et al. 2007; Ayala et al. 2009), ¹³C¹H₃-methionine (Gelis
23 et al. 2007; Stoffregen et al. 2012) and ¹³C¹H₃-threonine (Velyvis et al. 2012; Ayala et al. 2020).
24 On the other hand, as leucine, valine and isoleucine residues are at the end of irreversible
25 metabolic pathways in *E.coli*, precursors can be incorporated in the growth medium for their
26 cost-effective labelling. The first precursors introduced to label isoleucine or leucine and valine
27 residues were 2-keto acids: α-ketobutyrate (Gardner et al. 1997) and α-ketoisovalerate (Goto et
28 al. 1999; Hajduk et al. 2000; Gross et al. 2003), respectively. However, α-ketoisovalerate used
29 as a precursor for leucine and valine residues is leading to a non-stereospecific labelling of both
30 pro-*S* and pro-*R* ¹³C¹H₃ groups resulting in overcrowded spectra for high molecular weight
31 proteins, even when both sensitivity and resolution have been improved using a non-
32 stereospecific ¹³C¹H₃/¹²C²H₃ α-ketoisovalerate (Tugarinov and Kay 2004b).

33 To prevent peak overlaps and to facilitate studies of large molecular weight assemblies,
34 methyl labelled acetolactate has been used as an alternative precursor (Gans et al. 2010). This

1 latter enables the stereospecific $^{13}\text{C}^1\text{H}_3$ -labelling of valine and leucine methyl groups and
2 therefore halves the number of peaks observed whilst improving by two the sensitivity of the
3 spectrum as compared to labelling at 50% pro-*S* and 50% pro-*R* methyl moieties using
4 optimized $^{13}\text{C}^1\text{H}_3/^{12}\text{C}^2\text{H}_3$ α -ketoisovalerate (Tugarinov and Kay 2004b). This interesting
5 precursor also enhances the intensity of NOE cross peaks and increases the distance threshold
6 at which NOE cross peaks can be detected by 20 % (Gans et al. 2010).

7 However, despite the tremendous progress made in protocols to selectively introduce
8 protonated methyl groups in perdeuterated proteins, sequence specific assignment, essential for
9 analyzing a variety of NMR data, remains an important challenge for large molecular
10 assemblies. Several methods to solve the bottleneck of assignment of large proteins have been
11 developed including parallel mutagenesis strategies (Amero et al. 2011), structure based
12 approaches using the analysis of NOE cross peaks with various programs (Pritišanac et al.
13 2020), MAP-XSII (Xu and Matthews 2013), FLAMEnGO 2.0 (Chao et al. 2014), MAGMA
14 (Pritišanac et al. 2017), MAGIC (Monneau et al. 2017), MethylFLYA (Pritišanac et al. 2019),
15 MAUS (Nerli et al. 2021) or the “divide-and-conquer” approach (Gelís et al. 2007; Sprangers
16 and Kay 2007) which is based on separation of large proteins into smaller fragments, assigning
17 these and transferring the assignment back to the full-length protein. For proteins of moderate
18 molecular weight or fragments of large assemblies for which backbone assignment is available,
19 it is possible to connect methyl resonances to those of the backbone. This requires a sample
20 with $^{13}\text{C}^1\text{H}_3$ labelled methyl groups connected to the backbone by a linear ^{13}C -chain. With such
21 a sample, transfer from the assigned backbone to the methyl groups can be achieved using either
22 unidirectional transfer from methyl groups to HN using (HM)CM(CGCBNA)NH experiments
23 (Tugarinov and Kay 2003) or ‘out and back’ HCC relay triple resonance experiments
24 (Tugarinov and Kay 2003; Ayala et al. 2012; Mas et al. 2013).

25 A combination of these techniques to assign methyl groups in addition with a
26 stereospecific labelling, enhancing the sensitivity of the spectrum by a factor two and
27 significantly reducing signal overlap, should lead to straightforward leucine and valine methyl
28 group assignment. Labelling schemes, connecting non-stereospecifically both leucine and
29 valine methyl groups (Tugarinov and Kay 2003), or only pro-*R* methyl moieties (Mas et al.
30 2013; Kerfah et al. 2015a), to the assigned backbone are already available. However, with such
31 precursors additional samples are required either to stereospecifically assign the methyl group
32 (Tugarinov and Kay 2004a; Gans et al. 2010) or to link the pro-*S* methyl to the pro-*R* one (Mas
33 et al. 2013; Kerfah et al. 2015a). Here we introduce the synthesis of a new dissymmetric $^{13}\text{C}^2\text{H}$ -
34 labelled acetolactate, a precursor that allows to directly connect the assigned leucine and valine

1 backbone atoms to the pro-*S* methyl groups via a linear ^{13}C chain using only one sample. This
2 new labelling scheme has been applied to the N-terminal domain of human HSP90 (HSP90-
3 NTD) and we present here the full assignment of methyl moieties of this protein.

4
5
6
7
8
9
10
11
12
13
14
15
16
17
18
19
20
21
22
23
24
25
26
27
28
29
30
31
32
33
34

1 **Materials and Methods**

2 **Synthesis of 1, 2, 3-[¹³C₃]- 4, 4, 4-[²H₃]-acetolactate.**

3 a) Synthesis of ethyl 1, 2, 3-[¹³C₃]-3-oxo-butanoate. A solution of LiHMDS (7.80 g, 46.6
4 mmoles, 2.1 equiv.) in freshly dried THF (150 mL) was cooled to -78°C under argon. 1, 2-
5 [¹³C₂]-ethyl acetate (2.00 g, 22.2 mmoles, Cambridge Isotope Laboratory, CIL) was added
6 dropwise. The resulting solution was stirred at -78°C for 15 min, then 1-[¹³C]-acetyl chloride
7 (1.60 mL, 22.2 mmoles, 1 equiv., CIL) was added dropwise. The resulting mixture was stirred
8 at -78 °C for additional 30 min then quenched by addition of a 20% aqueous solution of ¹HCl
9 (15 mL). After 3 extractions with Et₂O, the organics were combined, washed with saturated
10 Na¹HCO₃ solution then dried over Na₂SO₄. Concentration under vacuum affords the desired
11 product (2.88g) which was used in the next step without further purification).

12 ¹H NMR:(C²HCl₃), δ: 4.21 (dq, O-CH₂, ³J(¹H-¹H) = 7.1 Hz, ³J(¹H-¹³C) = 3.2 Hz, 2H); 3.46 (dt,
13 ¹³C-¹³CH₂-¹³C, ²J(¹H-¹³C) = 6.5 Hz, ¹J(¹H-¹³C) = 130.1 Hz, 2H); 2.28 (dd, CH₃-¹³C, ³J(¹H-¹³C)
14 = 1.4 Hz, ²J(¹H-¹³C) = 6.1 Hz, 3H), 1.30 (t, OCH₂-CH₃, ³J(¹H-¹H) = 7.1 Hz, 3H).

15
16
17 b) Synthesis of ethyl 1, 2, 3-[¹³C₃]-2-[¹³C¹H₃]-3-oxo-butanoate. ¹³C¹H₃-I (752 mL, 11.99
18 μmoles, 1.1 equiv, CIL) was slowly added to a solution of ethyl 1, 2, 3-[¹³C₃]-3-oxo butanoate
19 (1.45 g, 10.90 mmoles) in EtO¹H (50 mL) cooled to 0°C before addition of K₂CO₃ (1.66 g,
20 11.99 mmoles, 1.1 equiv.). The resulting suspension was warmed to room temperature then
21 stirred for 18 h. The mixture was concentrated to the fifth before addition of a large volume of
22 Et₂O. Excess of K₂CO₃ was filtered off and the filtrate concentrated under vacuum to the fifth
23 before a further addition of Et₂O and a second filtration. Concentration under vacuum affords
24 the desired product (1.03 g) as a colorless oil which was used in the next step without further
25 purification.

26 ¹H NMR:(C²HCl₃), δ: 4.21 (dq, O-CH₂, ³J(¹H-¹H) = 7.1 Hz, ³J(¹H-¹³C) = 3.0 Hz, 2H); 3.50
27 (dm, ¹³C-¹³CH-¹³C, ¹J(¹H-¹³C) = 129.0 Hz, 1H); 2.24 (dd, CH₃-¹³C, ³J(¹H-¹³C) = 1.3 Hz, ²J(¹H-
28 ¹³C) = 6.0 Hz, 3H), 1.36 (dm, ¹³CH₃, ¹J(¹H-¹³C) = 129.0 Hz, 3H), 1.28 (t, OCH₂-CH₃, ³J(¹H-
29 ¹H) = 7.1 Hz, 3H).

30
31 c) Synthesis of ethyl 1, 2, 3-[¹³C₃]-2-[¹³C¹H₃]-2-[O¹H]-3-oxo-butanoate. To a solution of ethyl
32 1, 2, 3-[¹³C₃]-2-[¹³C¹H₃]-3-oxo butanoate (995 mg, 6.72 mmoles) in DMSO (8 mL), Cs₂CO₃
33 was added (440 mg, 1.35 mmoles, 0.2 equiv.). After O₂ bubbling for 15 min., P(OEt)₃ (233 mL,
34 1.35 mmoles, 0.2 equiv.) was added. The resulting solution was stirred under O₂ atmosphere

1 for 20 h. A large volume of Et₂O was then added followed by a saturated NaCl solution. The
2 resulting phases were separated and the aqueous one was extracted one more time with Et₂O.
3 The organics were combined, dried over Na₂SO₄ then concentrated under vacuum to obtain
4 ethyl 1, 2, 3-[¹³C₃], 2-[¹³C¹H₃], 2-[O¹H]-3-oxobutanoate as a yellow oil (1.142 g) and pure
5 enough to be used in the next step without further purification.

6 ¹H NMR:(C²HCl₃), δ: 4.25 (dq, O-CH₂, ³J(¹H-¹H) = 7.1 Hz, ³J(¹H-¹³C) = 3.2 Hz, 2H); 4.17-
7 4.24 (m, OH, 1H), 2.27 (dd, CH₃-¹³C, ³J(¹H-¹³C) = 1.1 Hz, ²J(¹H-¹³C) = 6.1 Hz, 3H), 1.36 (dm,
8 ¹³CH₃, ¹J(¹H-¹³C) = 134.2 Hz, 3H), 1.28 (t, OCH₂-CH₃, ³J(¹H-¹H) = 7.1 Hz, 3H).

9
10 d) Synthesis of sodium 1, 2, 3-[¹³C₃]-2-[¹³C¹H₃]-2-[O²H]-3-oxo-4, 4, 4-[²H₃]-butanoate. To a
11 solution of ethyl 1, 2, 3-[¹³C₃]- 2-[¹³C¹H₃]-2-[O¹H]-3-oxobutanoate (1.09 g) in ²H₂O (4 mL),
12 0.4 equivalents of a solution of NaO²H (2.5 M) in ²H₂O were added dropwise in 40 min, using
13 a syringe pump under argon. As soon as the addition was completed, ¹H NMR was carried out
14 on a sample (few μL) in ²H₂O in order to calculate the conversion percentage (*ratio* between
15 the amount of hydrolyzed product (quadruplet at 1.60 ppm) and the amount of starting material
16 (quadruplet at 1.7 ppm)). 1.1 equivalent of NaO²H solution (2.5 M) was added over 30 min
17 with the syringe pump. As soon as the addition was completed, an extraction with diethyl ether
18 was carried out in order to remove the by-product coming from the previous step whose NMR
19 signals prevent a good follow-up of the hydrogen/deuterium (¹H/²H) exchange on the 4-CH₃
20 (2.2 ppm). The ¹H/²H exchange on 4-CH₃ was then monitored by ¹H NMR and carried out by
21 successive addition of NaO²H (2.5 M) until the integral of the doublet corresponding to the CH₃
22 reaches the value of 0.1 when the quadruplet at 1.6 ppm integrates for 1.5. The reaction was
23 immediately neutralized with a concentrated ²HCl solution to neutral pH and then buffered with
24 Tris-¹HCl, (1.0 M, pH 7.5 in ²H₂O). The concentration of the resulting solution was then
25 determined by ¹H NMR using methanol or acetonitrile as internal reference. The final product
26 (3.02 mmoles) was stored at -80°C.

27 ¹H NMR:(C²HCl₃), δ: 1.37 (dq, ¹³CH₃, ¹J(¹H-¹³C) = 129.3 Hz, ²J(¹H-¹³C) = 3.9 Hz, 1H).

28

29 **Preparation of isotopically labelled HSP90-NTD samples.**

30 *E. coli* BL21-DE3-RIL cells transformed with a pET-28 plasmid encoding the N-Terminal
31 domain of HSP90 α from *Homo Sapiens* (HSP90-NTD) with a His-Tag and a TEV cleavage
32 site were progressively adapted in three stages over 24 h to M9/²H₂O. In the final culture,
33 bacteria were grown at 37°C in M9 medium with 99.85 % ²H₂O (Eurisotop), 1 g/L ¹⁵N¹H₄Cl

1 (Sigma Aldrich) and 2 g/L D-glucose-d₇ (for U-[²H, ¹²C, ¹⁵N] HSP90-NTD samples) or D-
2 glucose-¹³C₆-d₇ (CIL) (for U-[²H, ¹³C, ¹⁵N] HSP90-NTD samples).

3 For methyl specifically labelled samples, the methyl labelled precursors or amino-acids were
4 added to the media when the O.D at 600 nm reached 0.6 (Kerfah et al. 2015c):

- 5 - Labelling scheme (A): for production of the U-[²H, ¹⁵N, ¹³C], Ile-[2, 3, 4, 4-²H₄; 1, 2,
6 3, 4-¹³C₄; ¹³C¹H₃]^{δ1}/[¹²C²H₃]^{γ2}], Leu-[2, 3, 3, 4-²H₄; 1, 2, 3, 4-¹³C₄; [¹³C¹H₃]^{pro-S}/
7 [¹²C²H₃]^{pro-R}], Val-[2, 3-²H₂; 1, 2, 3-¹³C₃; [¹³C¹H₃]^{pro-S}/¹²C²H₃]^{pro-R}] HSP90-NTD, a
8 solution containing the sodium 1, 2, 3-[¹³C₃]-2-[¹³C¹H₃]-2-[O²H]-3-oxo-4, 4, 4-[²H₃]-
9 butanoate precursor was added at a concentration of 172 mg/L 1 h before induction. 40
10 min later (20 minutes before induction) a solution containing 60 mg/L of sodium (S)-2-
11 hydroxy-2-(1',1'-[²H₂], 1', 2'-[¹³C₂])ethyl-3-oxo-1,2,3-[¹³C₃]-4,4,4-[²H₃]butanoate
12 (Kerfah et al. 2015a) was added to the medium.
- 13 - Labelling scheme (B): for production of the U-[²H, ¹⁵N, ¹²C], Ala-[¹³C¹H₃]^β, Met-
14 [¹³C¹H₃]^ε, Leu/Val-[¹³C¹H₃]^{pro-S}, Ile-[¹³C¹H₃]^{δ1}, Thr-[¹³C¹H₃]^γ HSP90-NTD, a HLAM-
15 A^βI^{δ1}M^εLV^{proS}T^γ kit, purchased from NMR-Bio, was added before induction according
16 to the manufacturer's protocol.
- 17 - Labelling scheme (C): U-[²H, ¹⁵N, ¹²C] samples labelled on a single type of methyl
18 group were produced in small scales (21 mL) to identify A^β, M^ε, T^γ methyl type (3
19 samples) or to complete assignment using single point mutants (Amero et al. 2011) (33
20 samples, list of mutants presented in the legend of Fig. S4). Single point amino acid
21 mutations were generated by GeneCust. For each of these samples a single type of
22 methyl groups was labelled by addition of the corresponding NMR-Bio kit (SLAM-A^β,
23 SLAM-M^ε, SLAM-I^{δ1}, SLAM-T^γ or DLAM-LV^{proS}) in M9/²H₂O media 1 h before
24 induction.

25
26 Protein production was induced by the addition of IPTG to a final concentration of 0.5
27 mM. The cultures were grown overnight at 20°C before harvesting. Cells were collected by
28 centrifugation at 5500 g for 20 min at 4°C then lysed by sonication on ice in a buffer containing
29 20 mM phosphate sodium buffer at pH 7.4, 0.5 M NaCl, 0.05% β-ME, antiprotease (cOmplete®
30 EDTA free, 1 tablet for 50 mL), 50 μg/mL DNase (Sigma Aldrich), 50μg/mL RNase
31 (Euromedex), and 0.25 mg/mL Lysozyme (Euromedex). After removal of cell debris by
32 centrifugation (45,000×g, 30 min, 4 °C), the supernatant was purified using an affinity
33 chromatography step (Ni-NTA, Superflow, QIAGEN) (labelling scheme A, B and C), followed
34 by a size exclusion chromatography step (16/600 Superdex 75 PG, GE Healthcare) (labelling

1 schemes A and B only). The gel filtration column was run with an isocratic step of the NMR
2 buffer (20 mM Hepes, 150 mM NaCl, 1 mM TCEP, pH 7.5).

3 The HSP90-NTD proteins were concentrated, using an Amicon® 4 Centrifugal Filter
4 Unit with a 10,000 MWCO (Merck), either in a 90%/10% $^1\text{H}_2\text{O}/^2\text{H}_2\text{O}$ or in a 100% $^2\text{H}_2\text{O}$ buffer
5 containing 20 mM Hepes, 150 mM NaCl, 1 mM TCEP, pH 7.5. For labelling schemes A and
6 B, samples were concentrated to 0.5 mM and 200 μL of each sample was loaded in 4 mm
7 shigemi tube. The wild type and single point mutants of HSP90-NTD proteins labelled on only
8 one methyl type (labelling scheme C) were concentrated at [0.1-0.4] mM and 40 μL of each
9 sample was loaded in a 1.7 mm NMR tube.

10

11 NMR Spectroscopy

12 All NMR experiments acquired on HSP90-NTD samples were recorded at 298 K. 2D
13 ^1H - ^{13}C SOFAST methyl TROSY (Amero et al. 2009) experiments to identify each methyl type
14 as well as to assign individual methyl signals using single point mutants were recorded for an
15 average duration of ~ 1.5 h each, on a spectrometer operating at a ^1H frequency of 850 MHz
16 and equipped with a 1.7 mm cryogenically cooled, pulsed-field-gradient triple-resonance probe.
17 All other NMR experiments were acquired using Bruker Avance III HD spectrometers equipped
18 with 5 mm cryogenic probes (operating at a ^1H frequency of 600 or 950 MHz).

19 The 3D HCC, HC(C)C and HC(CC)C experiments (Tugarinov and Kay 2003; Ayala et
20 al. 2009, 2012; Mas et al. 2013) were acquired on a spectrometer operating at a ^1H frequency
21 of 600 MHz for a total duration of 4 days, using a 0.5 mM sample of U- ^2H , ^{15}N , ^{13}C , Ile-[2,
22 3, 4, 4- $^2\text{H}_4$; 1, 2, 3, 4- $^{13}\text{C}_4$; $^{13}\text{C}^1\text{H}_3$] $^{\delta 1}$ /[$^{12}\text{C}^2\text{H}_3$] $^{\gamma 2}$], Leu-[2, 3, 3, 4- $^2\text{H}_4$; 1, 2, 3, 4- $^{13}\text{C}_4$; [$^{13}\text{C}^1\text{H}_3$] $^{\text{pro-}}$
23 S /[$^{12}\text{C}^2\text{H}_3$] $^{\text{pro-R}}$], Val-[2, 3- $^2\text{H}_2$; 1, 2, 3- $^{13}\text{C}_3$; [$^{13}\text{C}^1\text{H}_3$] $^{\text{pro-S}}$ /[$^{12}\text{C}^2\text{H}_3$] $^{\text{pro-R}}$] HSP90-NTD. The
24 interscan delay was adjusted to 0.5-0.6 s, the heteronuclear $^1\text{H} \rightarrow ^{13}\text{C}$ transfer delay was set to
25 4 ms ($1/(2 \times ^1J_{\text{HC}})$) and the homonuclear $^{13}\text{C} \rightarrow ^{13}\text{C}$ transfer delay was fixed to 12.5 ms. The
26 acquisition times were adjusted to 8-10.7 ms in the ^{13}C indirect dimension, and to 70 ms in ^1H
27 direct dimension.

28 For the sequential assignment of backbone resonances, a set of 6 BEST-TROSY 3D
29 triple resonance experiments (HNCA, HN(CA)CB, HNCO, HN(CA)CO, HN(CO)CA and
30 HN(COCA)CB (Favier and Brutscher 2019) were acquired on a Bruker Avance III HD
31 spectrometer equipped with a cryogenic probe and operating at a ^1H frequency of 600 MHz for
32 a total duration of 11 days using a 0.5 mM sample of the U- ^2H , ^{15}N , ^{13}C] HSP90-NTD.

33 The 3D CCH HMQC-NOESY-HMQC NMR experiment (Tugarinov et al. 2005; Törner
34 et al. 2020) was recorded over 3 days on a spectrometer operating at a ^1H frequency of 950 MHz

1 using a 0.5 mM sample of U-[²H, ¹⁵N, ¹²C], Ala-[¹³C¹H₃]^β, Met-[¹³C¹H₃]^ε, Leu/Val-[¹³C¹H₃]^{pro-}
2 ^δ, Ile-[¹³C¹H₃]^{δ1}, Thr-[¹³C¹H₃]^γ HSP90-NTD. The interscan delay was set to 1.1s. The
3 heteronuclear ¹H -> ¹³C transfer delay was set to 4 ms (1/(2 x ¹J_{HC})). The acquisition times in
4 the ¹³C indirect dimension were set to 24.6 ms, (t_{1max}) and to 18.6 ms (t_{2max}). In the ¹H direct
5 dimension t_{3max} was fixed to 80 ms. The NOE mixing period was set to 500 ms to detect a
6 maximum number of long-range intermethyl NOEs.

8 **Data processing and analysis**

9 All data were processed and analyzed using nmrPipe/nmrDraw (Delaglio et al. 1995)
10 and CcpNMR (Vranken et al. 2005). Automated methyl assignment was performed using
11 MAGIC software (Monneau et al. 2017) using the reference structure of HSP90-NTD (PDB:
12 1YES). Input NOE lists for MAGIC were created with CcpNMR. MAGIC was run with a score
13 threshold factor of 1 and distance thresholds of 7–10 Å using all inter methyl NOEs detected
14 (S/N threshold of 5 was used) and given the assignment of isoleucines, leucines and valines
15 previously obtained by the three ‘out and back’ HCC experiments as well as alanine, methionine
16 and threonine methyl groups assigned by mutagenesis as additional input.

1 Results and Discussion

2
3 To assign methyl groups of large perdeuterated proteins, previously assigned backbone
4 resonances of these proteins can be used (Tugarinov and Kay 2003; Ayala et al. 2012; Mas et
5 al. 2013). Nonetheless, to do so, methyl groups need to be connected, via a linear chain of ^{13}C ,
6 to the backbone atoms in order to be able to apply optimized experiments to high molecular
7 weight proteins. Strategies to label stereospecifically leucine and valine pro-*R* methyl groups
8 and to connect them to backbone nuclei have already been proposed (Mas et al. 2013).
9 However, it has to be noted that pro-*S* methyl groups are often chosen over pro-*R* methyl groups
10 as they are both easier and cheaper to label stereospecifically (Gans et al. 2010). In order to
11 simplify assignment of pro-*S* methyl groups using already assigned backbone resonances and
12 to avoid the need of an additional sample to link the pro-*S* methyl to the pro-*R* one, a sample
13 connecting the pro-*S* $^{13}\text{C}^1\text{H}_3$ -methyl groups to the backbone atoms by a linear ^{13}C -chain and
14 labelled with $^{12}\text{C}^2\text{H}_3$ on pro-*R* methyl moieties to avoid signal loss would be optimal.

16 Synthesis of optimally labelled acetolactate precursors and proteins.

17 Taking into account the specificity of leucine/valine metabolic pathway in *E. coli*, such
18 an optimal labelling scheme can be achieved in $\text{M9}^2\text{H}_2\text{O}$ medium using $^{13}\text{C}^2\text{H}$ glucose (Kerfah
19 et al. 2015c) as a carbon source together with 1, 2, 3- $^{13}\text{C}_3$ -2- $^{13}\text{C}^1\text{H}_3$ -2- $[\text{O}^2\text{H}]$ -3-oxo-4, 4, 4-
20 $^2\text{H}_3$ -butanoate as suitably labelled acetolactate precursor. However, this latter cannot be
21 synthesized from commercially available materials by the traditional route starting from
22 acetoacetate (Gans et al. 2010) since the corresponding labelled starting material is not
23 commercially available. Indeed, acetolactate chemical synthesis is achieved by reaction of
24 iodomethane on acetoacetate (Gans et al. 2010). Whilst both $^{13}\text{C}^1\text{H}_3$ labelling of the methyl
25 substituent in position 2 and deuteration of the methyl group in position 4 can be obtained using
26 $^{13}\text{C}^1\text{H}_3\text{I}$ as a starting synthesis material and hydrogen/deuterium exchange in controlled basic
27 conditions (Gans et al. 2010), respectively, the ^{13}C labelling of only the first three carbons of
28 the main chain using commercially available labelled acetoacetate materials is not achievable.
29 Therefore, as acetoacetate can be obtained by condensation of two acetate moieties (Epstein J
30 et al. 1977), we decided to set up a synthesis of dissymmetrically labelled acetoacetate starting
31 from commercially available ethyl 1, 2- $^{13}\text{C}_2$ -acetate with 1- ^{13}C -acetyl chloride. Based on
32 reported procedures, we established a 4-step synthesis (Fig. 1) allowing to prepare the desired
33 precursor with an overall yield of 27%. In brief, the dissymmetry is achieved by the Claisen
34 condensation of ethyl-1,2, $^{13}\text{C}_2$ -acetate with 1- ^{13}C -acetyl chloride using an optimization of a

1 reported procedure (Epstein J et al. 1977) (a), followed by an alkylation in position 2 using
2 $^{13}\text{C}^1\text{H}_3\text{I}$ (b) and a subsequent hydroxylation in position 2 (c). Finally, the last step combining
3 both saponification of the ester and a hydrogen/deuterium exchange in position 4 is performed
4 under controlled basic conditions (d). This last step is very delicate and requires a fine control
5 of the basic condition as a methyl rearrangement above a pH of 13.5 can take place resulting in
6 the interconversion of both methyl groups (Gans et al. 2010). Steps (b) and (c) are not
7 stereoselective, hence, products of these latter steps were produced as racemic mixtures. The
8 optimally labelled acetolactate, unstable at room temperature, was aliquoted and stored at -
9 80°C .

10 The synthesized acetolactate precursor was incorporated in *E. coli*. $\text{M9}^2\text{H}_2\text{O}$ culture
11 media without any further purification steps to label the overexpressed protein. Frozen
12 acetolactate vials were thawed right before addition in the culture medium to avoid degradation
13 or methyl rearrangement. It has to be noted that only the 2-(*S*) stereoisomer of acetolactate is
14 converted *in vivo* by ketol–acid reductoisomerase (EC1.1.1.86) and dihydroxyacid dehydratase
15 (EC 4.2.1.9) to form the stereospecifically labelled 2-keto-isovalerate. This latter is afterwards
16 directly converted into valine or combined with $^{13}\text{C}^2\text{H}$ -pyruvate, derived from the $^{13}\text{C}^2\text{H}$ -
17 glucose, to produce leucine with the desired labelling pattern. The 2-(*R*) stereoisomer of
18 acetolactate is, itself, not a substrate of ketol–acid reductoisomerase and hence, induces no
19 scrambling (Gans et al. 2010). The synthesized 1, 2, 3- $^{13}\text{C}_3$ -2- $^{13}\text{C}^1\text{H}_3$ -2- $[\text{O}^2\text{H}]$ -3-oxo-4, 4, 4-
20 $^{2}\text{H}_3$ -butanoate can be mixed with other known precursors allowing also to connect methyl
21 groups, such as Ile- δ_1 (Kerfah et al. 2015b, a; Törner et al. 2020), Ile- γ_2 (Ayala et al. 2012) or
22 Ala- β (Ayala et al. 2009; Kerfah et al. 2015a; Törner et al. 2020), to backbone nuclei using a
23 linear ^{13}C chain. In this study, we chose to label our sample on both leucine/valine pro-*S* and
24 isoleucine- δ_1 methyl moieties, by adding Ile- δ_1 precursor (sodium (S)-2-hydroxy-2-(1',1'-
25 $^{2}\text{H}_2$], 1', 2'- $^{13}\text{C}_2$)ethyl-3-oxo-1,2,3- $^{13}\text{C}_3$ -4,4,4- $^{2}\text{H}_3$ -butanoate – (Kerfah et al. 2015a,b))
26 together with our new optimized acetolactate. The isoleucine precursor was added in the culture
27 medium 40 min later than the new precursor in order to take into account co-incorporation
28 incompatibilities between both the leucine/valine precursor and the isoleucine one. Indeed,
29 enzymes from ILV-pathway have a tendency to process preferentially isoleucine precursor
30 instead of leucine/valine precursors (Kerfah et al. 2015b, c). Incorporation of both precursors
31 during the protein expression did not lead to a significantly different HSP90-NTD yield with
32 regards to the yields obtained in standard $\text{M9}^2\text{H}_2\text{O}$ media. No scrambling was detected neither
33 to the pro-*R* methyls groups of leucine and valine nor to the isoleucine- γ_2 site (Fig. S1a).

34

1 **Connection of $I^{\delta^1}L^{\delta^2}V^{\gamma^2}$ methyl groups to C_α and C_β atoms.**

2 Using this new precursor, it is possible to directly correlate pro-*S* methyl groups of
3 leucine and valine residues to their respective C_α and C_β . We decided to apply this strategy to
4 the N-terminal domain of human HSP90 (HSP90-NTD), an extensively studied protein, whose
5 isoform assignment (α and β), including partial assignment of its methyl groups, is available
6 (Jacobs et al. 2006; Elif Karagöz et al. 2011; Park et al. 2011; Lescanne et al. 2017, 2018).
7 Here, we have focused on the N-terminal domain of the α isoform, a 29 kDa protein that
8 contains 20 isoleucine, 18 leucine and 11 valine residues. This dynamic protein is particularly
9 challenging to assign using automatic methyl assignment methods and reported success rates
10 are ranging from 27 % to 69 % (Pritišanac et al. 2017; Monneau et al. 2017; Pritišanac et al.
11 2019, 2020). In our hands, only 34 % of the methyl groups (30/87) could be assigned
12 automatically with 1) a single assignment, 2) a high NOE assignment completeness of the strip
13 related to each peak (> 50 %) and 3) a high total confidence score value (≥ 7) (Table S1) using
14 the HSP90-NTD X-ray structure (PDB: 1YES) and experimentally detected NOE network.
15 Therefore, this protein is a good candidate to assess our experimental strategy based on new
16 precursors.

17 To do so, 200 μ L at 0.5 mM of an optimally labelled sample was used to acquire three
18 ‘out and back’ HCC, HC(C)C and HC(CC)C experiments (Tugarinov and Kay 2003; Ayala et
19 al. 2009, 2012; Mas et al. 2013) connecting labelled $I^{\delta^1}L^{\delta^2}V^{\gamma^2}$ methyls groups to $I^{\gamma^1}L^{\gamma}V^\beta$, $I^\beta L^\beta V^\alpha$
20 and $I^\alpha L^\alpha$ resonances. 100 % and 94 % of the expected C_β and C_α coherences, respectively, were
21 observed for the 29 kDa HSP90-NTD at 298 K (τ_C *c.a.* 20 ns) (Fig. 2). The three missing C_α
22 resonances correspond to residues L56, I26 and I110, two of them being affected by extensive
23 line broadening due to conformational exchange. With such a high percentage of observed C_α
24 and C_β resonances we demonstrate the applicability of this method for medium size proteins.
25 In order to validate the strategy for larger proteins, the labelling scheme was applied to the 87
26 kDa hetero hexameric protein prefoldin from *Pyrococcus horikoshii*, containing 2 α and 4 β -
27 subunits. Only the β -subunits were labelled with the optimal labelling schemes described above,
28 whilst the α -subunits remained perdeuterated (Fig. S1b). Three HCC experiments were
29 collected on this 0.2 mM sample of prefoldin at 310 K (τ_C *c.a.* 60 ns). 95% and 60% of the
30 expected C_β and C_α coherences, respectively, were observed (Fig. S2) despite the high
31 molecular weight of the protein and the presence of doubled peaks due to the presence of two
32 inequivalent β -subunits in the $\alpha_2\beta_4$ hexameric prefoldin (Ohtaki et al. 2008). Such HCC
33 experiments were also acquired at 343 K (τ_C *c.a.* 30 ns) on this hyperthermophilic prefoldin

1 sample, enabling transfer of assignment between backbone atoms and methyl groups (Törner
2 et al. 2021).

3

4 **Application to the sequence specific assignment of $I^{\delta 1}L^{\delta 2}V^{\gamma 2}$ methyl groups of HSP90-NTD**

5 Backbone sequential assignment was performed using 6 ‘BEST-TROSY’ triple
6 resonance experiments (Favier and Brutscher 2019). C_{α} and C_{β} resonances were assigned for
7 89 % and 80 % of the residues of HSP90-NTD respectively, excluding the loosely structured
8 N-terminal [1-16] and C-terminal [225-236] regions. The segment L103-T115, that covers the
9 ligand binding site, is invisible by NMR due to dynamics in the μ s-ms timescale. Transfer of
10 sequentially assigned backbones resonances to isoleucine- δ_1 , leucine- δ_2 and valine- γ_2 methyl
11 groups was achieved using ‘out and back’ HCC experiments acquired on a U- $[^2H, ^{15}N, ^{13}C]$,
12 Ile-[2, 3, 4, 4- 2H_4 ; 1, 2, 3, 4- $^{13}C_4$; $^{13}C^1H_3$] $^{\delta 1}/[^{12}C^2H_3]^{\gamma 2}$], Leu-[2, 3, 3, 4- 2H_4 ; 1, 2, 3, 4- $^{13}C_4$;
13 $[^{13}C^1H_3]^{pro-S}/[^{12}C^2H_3]^{pro-R}$], Val-[2, 3- 2H_2 ; 1, 2, 3- $^{13}C_3$; $[^{13}C^1H_3]^{pro-S}/[^{12}C^2H_3]^{pro-R}$] labelled
14 HSP90-NTD sample. 2D extracts from the HCC experiments were compared with the
15 corresponding ones from the 3D HNCA and HN(CA)CB experiments and using C_{α} and C_{β}
16 resonances, all the $I^{\delta 1}L^{\delta 2}V^{\gamma 2}$ methyl groups could be unambiguously connected to previously
17 assigned backbone atoms (Fig. 2). The assignment was transferred in one step, very simply and
18 efficiently without having to correct for the isotopic shifts (Kerfah et al. 2015a). One must note
19 that the methyl- δ_1 of Ile-33 and Ile-128 are superimposed in the 2D methyl-TROSY spectrum,
20 but were unambiguously connected to the C_{α} resonances of both amino acids (Fig. S3).
21 Remained unassigned only methyl groups of L103, I104, L107 and I110 for which backbone
22 atoms are NMR-invisible due to extensive conformational exchange. Therefore, single point
23 mutagenesis was used to assign three of these last four $I^{\delta 1}$ or $L^{\delta 2}$ resonances (I104, L107 and
24 I110) (Fig. 3). The remaining residue, L103, was assigned by a careful re-analysis of both HCC
25 and backbone triple resonance experiments performed after the assignment of I104.

26

27 **Sequence specific assignment of $A^{\beta}M^{\epsilon}T^{\gamma}$ methyl groups of HSP90-NTD**

28 In the previous U- $[^2H, ^{15}N, ^{13}C]$, Ile-[2, 3, 4, 4- 2H_4 ; 1, 2, 3, 4- $^{13}C_4$; $^{13}C^1H_3$] $^{\delta 1}/[^{12}C^2H_3]^{\gamma 2}$],
29 Leu-[2, 3, 3, 4- 2H_4 ; 1, 2, 3, 4- $^{13}C_4$; $[^{13}C^1H_3]^{pro-S}/[^{12}C^2H_3]^{pro-R}$], Val-[2, 3- 2H_2 ; 1, 2, 3- $^{13}C_3$;
30 $[^{13}C^1H_3]^{pro-S}/[^{12}C^2H_3]^{pro-R}$] HSP90-NTD sample, only $I^{\delta 1}L^{\delta 2}V^{\gamma 2}$ methyl groups were connected
31 to backbone by a linear ^{13}C -chain. We did not incorporate labelled alanine in HSP90-NTD
32 culture for the sample used to acquire the HCC experiments although it is commercially
33 available with an optimal labelling pattern (1, 2, 3- $^{13}C_3$, 2- 2H -Ala). We recommend for future
34 studies to incorporate labelled alanine in the culture medium to decrease the numbers of mutants

1 required to complete the assignment. Regarding methionine and threonine residues, their
2 assignment cannot be undertaken using HCC experiments. Indeed, the sulfur atom present on
3 methionine residues prevents the use of HCC experiments to assign methionine methyl moieties
4 from available backbone assignment and the Thr-[1, 2, 3- ^{13}C , 2, 3- $^2\text{H}_2$, $^{13}\text{C}^1\text{H}_3$ - γ] labelled amino
5 acid is not commercially available impeding the use of HCC 3D experiments to transfer
6 assignment from backbone to threonine methyl groups in large proteins. Therefore, in order to
7 assign the remaining 38 A^β , M^ϵ and T^γ methyl groups, we decided to use a combination of both
8 single point mutations and through space intermethyl NOE correlation peaks. To assign the
9 remaining A^β , M^ϵ and T^γ methyl groups using inter-methyl NOE-connectivities a U-[^2H , ^{15}N ,
10 ^{12}C], Ala-[$^{13}\text{C}^1\text{H}_3$] $^\beta$, Met-[$^{13}\text{C}^1\text{H}_3$] $^\epsilon$, Leu/Val-[$^{13}\text{C}^1\text{H}_3$] $^{\text{pro-S}}$, Ile-[$^{13}\text{C}^1\text{H}_3$] $^{\delta 1}$, Thr-[$^{13}\text{C}^1\text{H}_3$] $^\gamma$ HSP90-
11 NTD sample was required. Indeed, intermethyl NOE connectivities between previously
12 assigned isoleucine, leucine and valine residues and unassigned A^β , M^ϵ and T^γ methyl groups
13 simplify the assignment of methionine, threonine and alanine methyl moieties.

14 First small-scale samples with only one type of methyl group labelled A^β , M^ϵ or T^γ were
15 prepared to identify the amino acids type corresponding to each correlation remaining to assign
16 in the 2D methyl-TROSY spectrum. Then, we overexpressed and purified in small scale 30
17 single point $^{13}\text{C}^1\text{H}_3$ -labelled mutants. In order to minimize secondary chemical shifts
18 replacement amino acids that were structurally similar to the substituted amino acid were
19 chosen (Crublet et al. 2014) (Fig. S4).

20 Each of these samples containing 100 to 500 μg of $^{13}\text{C}^1\text{H}_3$ -labelled single point mutant
21 of HSP90-NTD were used to acquire a 2D SOFAST-methyl-TROSY spectrum (Amero et al
22 2009; Amero et al 2011) on a NMR spectrometer operating at a ^1H frequency of 850 MHz and
23 equipped with a sample changer and a 1.7 mm cryogenic probe head. This mutant library
24 allowed us to assign unambiguously 27 methyl groups. Three spectra of single point mutants
25 were more complex to analyze due to chemical shift perturbations that result from the
26 introduced mutation (Fig. S5). Out of the 38 A^β , M^ϵ and T^γ methyl groups, eleven remained
27 unassigned after the first analysis of the mutant library, among them eight methyls (one M^ϵ , two
28 A^β and five T^γ methyl groups) for which mutants were not available and three T^γ methyl groups
29 whose mutant spectra were challenging to analyze. The sole unassigned methionine methyl
30 signal was unambiguously assigned as the last remaining methionine residue (M98).

31 To complete the assignment for the last 10 methyl groups, a 0.5 mM sample of U-[^2H ,
32 ^{15}N , ^{12}C], Ala-[$^{13}\text{C}^1\text{H}_3$] $^\beta$, Met-[$^{13}\text{C}^1\text{H}_3$] $^\epsilon$, Leu/Val-[$^{13}\text{C}^1\text{H}_3$] $^{\text{proS}}$, Ile-[$^{13}\text{C}^1\text{H}_3$] $^{\delta 1}$, Thr-[$^{13}\text{C}^1\text{H}_3$] $^\gamma$
33 labelled HSP90-NTD was prepared to acquire a 3D HMQC-NOESY-HMQC. A total of 344
34 intermethyl NOEs cross peaks with a $\text{S/N} \geq 5$ were detected between methyls distant by up to

1 10 Å. Examples of intermethyl NOE and a matrix presenting all the observed NOEs are
2 displayed in Fig. 4. To assign the remaining 2 alanines and 8 threonines, the NOE connectivities
3 and the previously assigned methyls (49 I^{δ1}L^{δ2}V^{γ2} and 28 A^βM^ε and T^γ methyl groups) were
4 used as input for the program MAGIC. Six methyl groups (2 alanines (A141 and A145) and 4
5 threonines (T90, T88, T115 and T149)) were unambiguously assigned with both a high
6 percentage of NOE correlation peaks assigned and a high confidence score. Four threonines
7 (T94, T109, T176 and T184) were left either with multiple assignments or an assignment with
8 a low confidence score. However, taking into account the information obtained from the NOE-
9 based assignment, the mutant spectra displaying chemical shift perturbations (Fig. S5) were
10 carefully reanalyzed allowing us to assign the four remaining threonine methyl signals.

11 Finally, all the 87 methyl groups of HSP90-NTD were assigned using both isoleucine
12 precursor and the newly labelled acetolactate for isoleucine, leucine and valine methyl groups
13 and this mixed NOE/mutants strategy for alanine, methionine and threonine methyl moieties
14 (Fig. 5, Table S2). It can be noted that, there is, indeed, an overlap of two isoleucines (I33/I128)
15 explaining only 86 visible peaks. Even though dynamics in the intermediate regime broaden
16 the backbone resonances of the segment which is covering the ATP binding site [103-115]
17 beyond the detection threshold, the according methyl probes are visible. The assignment of
18 L103, I104, L107, T109, I110, A111 and T115 render this previously invisible region amenable
19 to NMR studies.

20
21
22
23
24
25
26
27
28
29
30
31
32
33
34

1 **Conclusion:**

2
3 This research reports the synthesis of a new dissymmetric $^{13}\text{C}/^2\text{H}$ -labelled acetolactate, a
4 precursor that allows to connect directly, via linear ^{13}C chains, backbone atoms to the pro-*S*
5 methyl groups of leucine and valine residues. This optimized precursor can be combined with
6 isoleucine precursor and $^2\text{H}/^{13}\text{C}$ -alanine to enable the transfer of assignment from backbone to
7 methyl groups with only one sample without requiring the correction of $^1\text{H}/^2\text{H}$ isotopic chemical
8 shift for the ^{13}C resonances. We expect that this new precursor will ease the assignment of
9 leucine and valine pro-*S* methyl groups of proteins using already assigned backbone resonances
10 as it simplifies the analysis of the NMR experiments. This innovative labelling scheme was
11 applied to the 29 kDa N-terminal domain of human HSP90 protein and to the 87 kDa hetero
12 hexameric prefoldin complex. Using both isoleucine precursor and the newly labelled
13 acetolactate, we managed to simply and efficiently transfer the backbone sequential assignment
14 to all the isoleucine- δ_1 , leucine and valine pro-*S* methyl moieties of HSP90-NTD. This allowed
15 us to confirm or correct the residue specific assignment of most isoleucine, leucine and valine
16 methyl groups (2 assignments were corrected for the 49 ILV residues – Table S2) and the
17 stereospecific assignment of prochiral methyl groups (5 stereospecific assignments were
18 inverted for the 29 leucine and valine residues – Table S2). In addition to the full assignment
19 of $\text{I}^{\delta_1}\text{L}^{\delta_2}\text{V}^{\gamma_2}$ methyl groups, we have used a mixed strategy based on mutagenesis and
20 intermethyl NOEs to assign 38 new methyl resonances corresponding to the $\text{A}^{\beta}\text{M}^{\epsilon}\text{T}^{\gamma}$ methyl
21 moieties of HSP90-NTD. Hence, we show that, despite extended conformational exchange that
22 impedes the complete backbone assignment, we managed to detect and assign signals for all
23 methyl probes including the ones belonging to the segment covering HSP90 ATP binding site.

24
25
26
27
28
29
30
31
32
33
34
35
36
37
38
39

1 **Data availability**

2

3 The FIDs acquired for this study are available in the biological magnetic resonance databank
4 (bmrbig12) and the assignment have been deposited under the BMRB ID: 50786.

5

6

7 **Acknowledgments**

8 The authors thank Dr. R Awad and Mr. L. Imbert for advice and stimulating discussions. This
9 work used the high field NMR and isotopic labelling facilities at the Grenoble Instruct-ERIC
10 Center (ISBG; UMS 3518 CNRS-CEA-UGA-EMBL) within the Grenoble Partnership for
11 Structural Biology (PSB). Platform access was supported by FRISBI (ANR-10-INBS-05-02)
12 and GRAL, a project of the University Grenoble Alpes graduate school (Ecoles Universitaires
13 de Recherche) CBH-EUR-GS (ANR-17-EURE-0003). IBS acknowledges integration into the
14 Interdisciplinary Research Institute of Grenoble (IRIG, CEA). This work was supported by
15 grants from CEA/NMR-Bio (research program C24990) and by the French National Research
16 Agency in the framework of the "*Investissements d'avenir*" program (ANR-15-IDEX-02).

17

18

19

20

21

22

23

24

25

26

27

28

29

30

31

32

33

34

35

36

37

38

39

40

41

42

43

1 **References**

- 2
- 3 Amero C, Asunción Durá M, Noirclerc-Savoie M, et al (2011) A systematic mutagenesis-
4 driven strategy for site-resolved NMR studies of supramolecular assemblies. *J Biomol*
5 *NMR* 50:229–236. <https://doi.org/10.1007/s10858-011-9513-5>
- 6 Amero C, Schanda P, Asunción Durá M, et al (2009) Fast Two-Dimensional NMR
7 Spectroscopy of High Molecular Weight Protein Assemblies. *J Am Chem Soc* 131:3448–
8 3449. <https://doi.org/10.1021/ja809880p>
- 9 Ayala I, Chiari L, Kerfah R, et al (2020) Asymmetric Synthesis of Methyl Specifically Labelled
10 L-Threonine and Application to the NMR Studies of High Molecular Weight Proteins.
11 *ChemistrySelect* 5:5092–5098. <https://doi.org/10.1002/slct.202000827>
- 12 Ayala I, Hamelin O, Amero C, et al (2012) An optimized isotopic labelling strategy of
13 isoleucine- γ 2 methyl groups for solution NMR studies of high molecular weight proteins.
14 *Chem Commun* 48:1434–1436. <https://doi.org/10.1039/c1cc12932e>
- 15 Ayala I, Sounier R, Usé N, et al (2009) An efficient protocol for the complete incorporation of
16 methyl-protonated alanine in perdeuterated protein. *J Biomol NMR* 43:111–119.
17 <https://doi.org/10.1007/s10858-008-9294-7>
- 18 Chao F-A, Kim J, Xia Y, et al (2014) FLAMEnGO 2.0: An enhanced fuzzy logic algorithm for
19 structure-based assignment of methyl group resonances. *J Magn Reson* 245:17–23.
20 <https://doi.org/10.1016/j.jmr.2014.04.012>
- 21 Crublet E, Kerfah R, Mas G, et al (2014) A cost-effective protocol for the parallel production
22 of libraries of CH₃-specifically labeled mutants for NMR studies of high molecular weight
23 proteins. *Methods Mol Biol* 1091:229–243. [https://doi.org/10.1007/978-1-62703-691-
24 7_17](https://doi.org/10.1007/978-1-62703-691-7_17)
- 25 Delaglio F, Grzesiek S, Vuister GW, et al (1995) NMRPipe: A multidimensional spectral
26 processing system based on UNIX pipes. *J Biomol NMR* 6:277–293.
27 <https://doi.org/10.1007/BF00197809>
- 28 Elif Karagöz G, Duarte AMS, Ippel H, et al (2011) N-terminal domain of human Hsp90 triggers
29 binding to the cochaperone p23. *108:580–585*. [https://doi.org/10.1073/pnas.1011867108/-
30 /DCSupplemental](https://doi.org/10.1073/pnas.1011867108/-/DCSupplemental)
- 31 Epstein J, Cannon P, Swidler R, Baraze A (1977) Amplification of cyanide ion production by
32 the micellar reaction of keto oximes with phosphono- and phosphorofluoridates. *J Org*
33 *Chem* 42:759–762. <https://doi.org/10.1021/jo00424a043>
- 34 Favier A, Brutscher B (2019) NMRlib: user-friendly pulse sequence tools for Bruker NMR

1 spectrometers. *J Biomol NMR* 73:199–211. <https://doi.org/10.1007/s10858-019-00249-1>

2 Gans P, Hamelin O, Sounier R, et al (2010) Stereospecific isotopic labeling of methyl groups
3 for NMR spectroscopic studies of high-molecular-weight proteins. *Angew Chemie - Int*
4 *Ed* 49:1958–1962. <https://doi.org/10.1002/anie.200905660>

5 Gardner KH, Kay LE, Chinchilla D, Fisher K (1997) Production and Incorporation of ^{15}N ,
6 ^{13}C , ^2H (^1H - δ^1 Methyl) Isoleucine into Proteins for Multidimensional NMR Studies.
7 *J Am Chem Soc* 119:7599–7600

8 Gauto DF, Estrozi LF, Schwieters CD, et al (2019) Integrated NMR and cryo-EM atomic-
9 resolution structure determination of a half-megadalton enzyme complex. *Nat Commun*
10 10:2697: <https://doi.org/10.1038/s41467-019-10490-9>

11 Gelis I, Bonvin AMJJ, Keramisanou D, et al (2007) Structural basis for signal sequence
12 recognition by the 204-kDa translocase motor SecA determined by NMR. *Cell* 131:756–
13 769. <https://doi.org/10.1016/j.cell.2007.09.039>

14 Goto NK, Gardner KH, Mueller GA, et al (1999) A robust and cost-effective method for the
15 production of Val, Leu, Ile (δ^1) methyl-protonated ^{15}N -, ^{13}C -, ^2H -labeled proteins. *J*
16 *Biomol NMR* 13:369–374

17 Gross JD, Gelev VM, Wagner G (2003) A sensitive and robust method for obtaining
18 intermolecular NOEs between side chains in large protein complexes. *J Biomol NMR*
19 25:235–242

20 Hajduk PJ, Augeri DJ, Mack J, et al (2000) NMR-based screening of proteins containing
21 ^{13}C -labeled methyl groups. *J Am Chem Soc* 122:7898–7904.
22 <https://doi.org/10.1021/ja0003501>

23 Isaacson RL, Simpson PJ, Liu M, et al (2007) A new labeling method for methyl transverse
24 relaxation-optimized spectroscopy NMR spectra of alanine residues. *J Am Chem Soc*
25 129:15428–15429. <https://doi.org/10.1021/ja0761784>

26 Jacobs DM, Langer T, Elshorst B, et al (2006) NMR Backbone Assignment of the N-terminal
27 Domain of Human HSP90. *J. Biomol. NMR* 36:52

28 Kerfah R, Hamelin O, Boisbouvier J, Marion D (2015a) CH_3 -specific NMR assignment of
29 alanine, isoleucine, leucine and valine methyl groups in high molecular weight proteins
30 using a single sample. *J Biomol NMR* 63:389–402. [https://doi.org/10.1007/s10858-015-](https://doi.org/10.1007/s10858-015-9998-4)
31 [9998-4](https://doi.org/10.1007/s10858-015-9998-4)

32 Kerfah R, Plevin MJ, Pessey O, et al (2015b) Scrambling free combinatorial labeling of
33 alanine- β , isoleucine- δ^1 , leucine-proS and valine-proS methyl groups for the detection of
34 long range NOEs. *J Biomol NMR* 61:73–82. <https://doi.org/10.1007/s10858-014-9887-2>

- 1 Kerfah R, Plevin MJ, Sounier R, et al (2015c) Methyl-specific isotopic labeling: a molecular
2 tool box for solution NMR studies of large proteins. *Curr Opin Struct Biol* 32:113–122.
3 <https://doi.org/10.1016/j.sbi.2015.03.009>
- 4 Lapinaite A, Simon B, Skjaerven L, et al (2013) The structure of the box C/D enzyme reveals
5 regulation of RNA methylation. *Nature* 502:519–523.
6 <https://doi.org/10.1038/nature12581>
- 7 Lescanne M, Ahuja P, Blok A, et al (2018) Methyl group reorientation under ligand binding
8 probed by pseudocontact shifts. *J Biomol NMR* 71:275–285.
9 <https://doi.org/10.1007/s10858-018-0190-5>
- 10 Lescanne M, Skinner SP, Blok A, et al (2017) Methyl group assignment using pseudocontact
11 shifts with PARAssign. *J Biomol NMR* 69:183–195. [https://doi.org/10.1007/s10858-](https://doi.org/10.1007/s10858-017-0136-3)
12 [017-0136-3](https://doi.org/10.1007/s10858-017-0136-3)
- 13 Mas G, Crublet E, Hamelin O, et al (2013) Specific labeling and assignment strategies of valine
14 methyl groups for NMR studies of high molecular weight proteins. *J Biomol NMR*
15 57:251–262. [https://doi.org/10.1007/s10858-](https://doi.org/10.1007/s10858-013-9785-z)
16 [013-9785-z](https://doi.org/10.1007/s10858-013-9785-z)
- 17 Mas G, Guan J-Y, Crublet E, et al (2018) Structural investigation of a chaperonin in action
18 reveals how nucleotide binding regulates the functional cycle. *Sci Adv* 4:eaau:4196.
19 <https://doi.org/doi:10.1126/sciadv.aau4196>
- 20 Monneau YR, Rossi P, Bhaumik A, et al (2017) Automatic methyl assignment in large proteins
21 by the MAGIC algorithm. *J Biomol NMR* 69:215–227. [https://doi.org/10.1007/s10858-](https://doi.org/10.1007/s10858-017-0149-y)
22 [017-0149-y](https://doi.org/10.1007/s10858-017-0149-y)
- 23 Nerli S, De Paula VS, McShan AC, Sgourakis NG (2021) Backbone-independent NMR
24 resonance assignments of methyl probes in large proteins. *Nat Commun* 12:691.
25 <https://doi.org/10.1038/s41467-021-20984-0>
- 26 Ohtaki A, Kida H, Miyata Y, et al (2008) Structure and Molecular Dynamics Simulation of
27 Archaeal Prefoldin: The Molecular Mechanism for Binding and Recognition of Nonnative
28 Substrate Proteins. *J Mol Biol* 376:1130–1141. <https://doi.org/10.1016/j.jmb.2007.12.010>
- 29 Park SJ, Kostic M, Dyson HJ (2011) Dynamic interaction of Hsp90 with its client protein p53
30 411(1):158-173. *J Mol Biol*. <https://doi.org/10.1016/j.jmb.2011.05.030>
- 31 Pritišanac I, Alderson TR, Güntert P (2020) Automated assignment of methyl NMR spectra
32 from large proteins. *Prog Nucl Magn Reson Spectrosc* 118–119:54–73.
33 <https://doi.org/10.1016/j.pnmrs.2020.04.001>
- 34 Pritišanac I, Degiacomi MT, Alderson TR, et al (2017) Automatic Assignment of Methyl-
NMR Spectra of Supramolecular Machines Using Graph Theory. *J Am Chem Soc*

1 139:9523–9533. <https://doi.org/10.1021/jacs.6b11358>

2 Pritišanac I, Würz JM, Alderson TR, Güntert P (2019) Automatic structure-based NMR
3 methyl resonance assignment in large proteins. *Nat Commun* 10:4922:
4 <https://doi.org/10.1038/s41467-019-12837-8>

5 Rosenzweig R, Moradi S, Zarrine-Afsar A, et al (2013) Unraveling the Mechanism of Protein
6 Disaggregation Through a ClpB-DnaK Interaction. *Science* (80-) 339:1080–1083.
7 <https://doi.org/10.1126/science.1233066>

8 Sounier R, Blanchard L, Wu Z, Boisbouvier J (2007) High-accuracy distance measurement
9 between remote methyls in specifically protonated proteins. *J Am Chem Soc* 129:472–
10 473. <https://doi.org/10.1021/ja067260m>

11 Sprangers R, Kay LE (2007) Quantitative dynamics and binding studies of the 20S proteasome
12 by NMR. *Nature* 445:618–622. <https://doi.org/10.1038/nature05512>

13 Stoffregen MC, Schwer MM, Renschler FA, Wiesner S (2012) Methionine scanning as an
14 NMR tool for detecting and analyzing biomolecular interaction surfaces. *Structure*
15 20:573–581. <https://doi.org/10.1016/j.str.2012.02.012>

16 Törner R, Awad R, Gans P, et al (2020) Spectral editing of intra- and inter-chain methyl–methyl
17 NOEs in protein complexes. *J Biomol NMR* 74:83–94. [https://doi.org/10.1007/s10858-](https://doi.org/10.1007/s10858-019-00293-x)
18 [019-00293-x](https://doi.org/10.1007/s10858-019-00293-x)

19 Törner R, Henot F, Awad R, et al (2021) Backbone and methyl resonances assignment of the
20 87 kDa prefoldin from *Pyrococcus horikoshii*. *Biomol NMR Assignment*.
21 <https://doi.org/10.1007/s12104-021-10029-4>

22 Tugarinov V, Hwang PM, Ollerenshaw JE, Kay LE (2003) Cross-correlated relaxation
23 enhanced ¹H-¹³C NMR spectroscopy of methyl groups in very high molecular weight
24 proteins and protein complexes. *J Am Chem Soc* 125:10420–10428.
25 <https://doi.org/10.1021/ja030153x>

26 Tugarinov V, Kay LE (2003) Ile, Leu, and Val Methyl Assignments of the 723-Residue Malate
27 Synthase G Using a New Labeling Strategy and Novel NMR Methods. *J Am Chem Soc*
28 125:13868–13878. <https://doi.org/10.1021/ja030345s>

29 Tugarinov V, Kay LE (2004a) Stereospecific NMR assignments of prochiral methyls, rotameric
30 states and dynamics of valine residues in malate synthase G. *J Am Chem Soc* 126:9827–
31 9836. <https://doi.org/10.1021/ja048738u>

32 Tugarinov V, Kay LE (2004b) An isotope labeling strategy for methyl TROSY spectroscopy.
33 *J Biomol NMR* 28:165–172

34 Tugarinov V, Kay LE, Ibraghimov I, Orekhov VY (2005) High-resolution four-dimensional

1 1H-13C NOE spectroscopy using methyl-TROSY, sparse data acquisition, and
2 multidimensional decomposition. *J Am Chem Soc* 127:2767–2775.
3 <https://doi.org/10.1021/ja044032o>

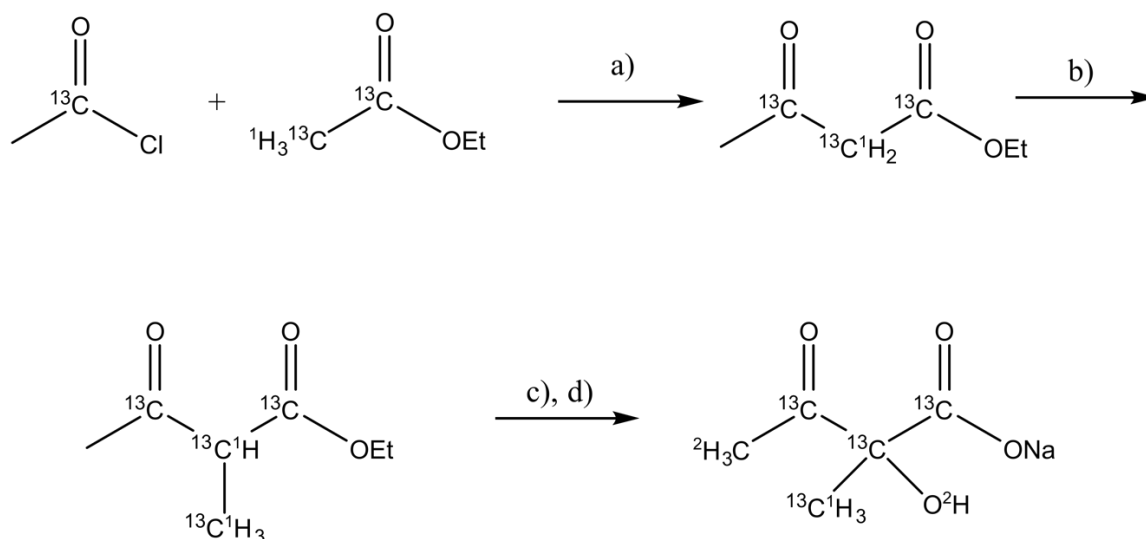
4 Velyvis A, Ruschak AM, Kay LE (2012) An Economical Method for Production of 2H,13CH3-
5 Threonine for Solution NMR Studies of Large Protein Complexes: Application to the 670
6 kDa Proteasome. *PLoS One* 7:e43725 <https://doi.org/10.1371/journal.pone.0043725>

7 Vranken WF, Boucher W, Stevens TJ, et al (2005) The CCPN data model for NMR
8 spectroscopy: Development of a software pipeline. *Proteins Struct Funct Genet* 59:687–
9 696. <https://doi.org/10.1002/prot.20449>

10 Xu Y, Matthews S (2013) MAP-XSII: An improved program for the automatic assignment of
11 methyl resonances in large proteins. *J Biomol NMR* 55:179–187.
12 <https://doi.org/10.1007/s10858-012-9700-z>

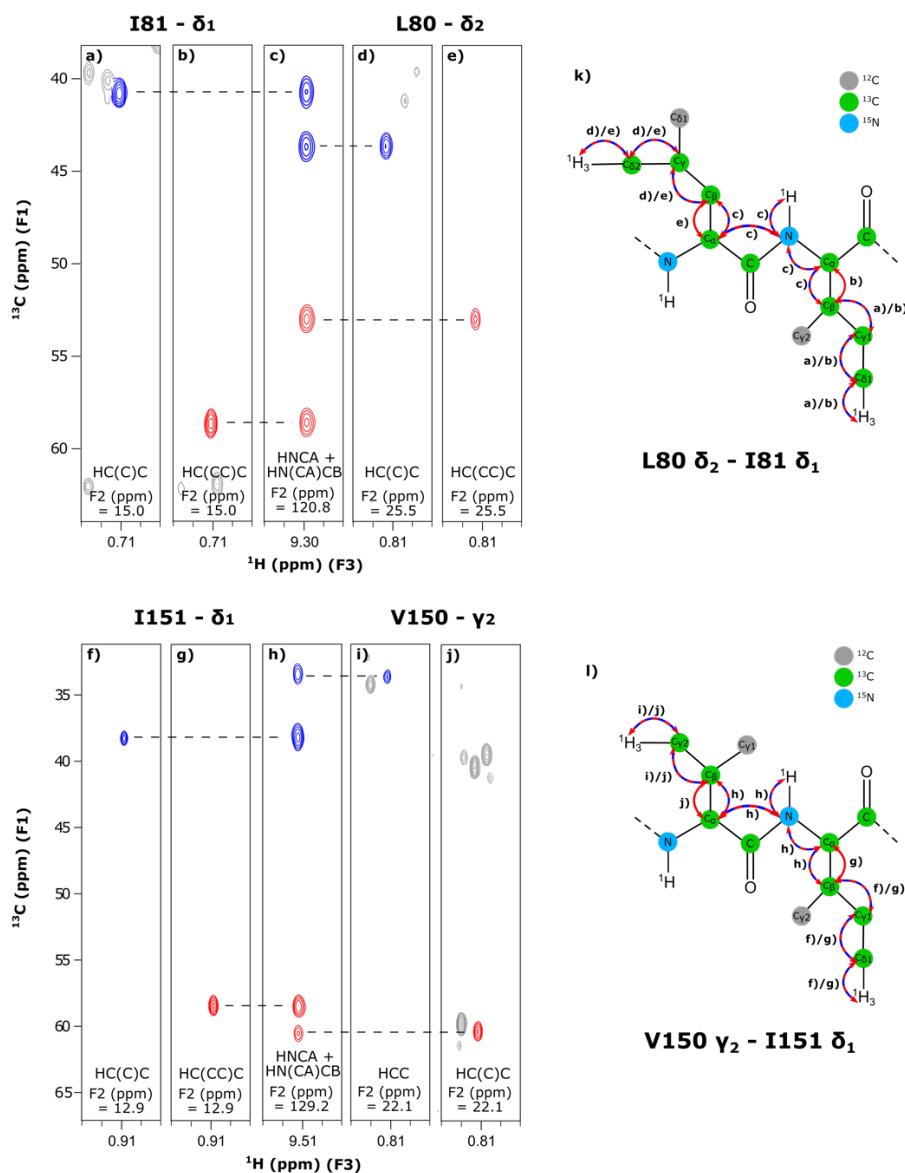
13
14
15
16
17
18
19
20
21
22
23
24
25
26
27
28
29
30
31
32
33
34
35
36
37
38
39
40
41
42
43
44

1
2
3
4
5
6
7



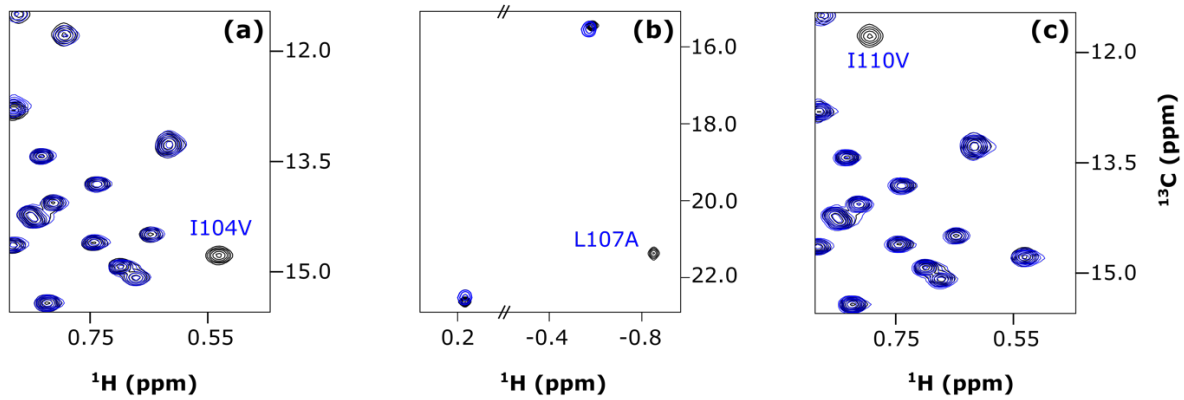
8
9
10
11
12
13
14
15
16
17
18
19
20
21
22
23
24
25
26
27
28

Fig. 1 Synthetic scheme for preparation of specifically labelled sodium 1, 2, 3- $^{13}\text{C}_3$ -2- $^{13}\text{C}^1\text{H}_3$ -2- $[\text{O}^2\text{H}]$ -3-oxo-4, 4, 4- $^2\text{H}_3$ -butanoate. **a)** i-LiHMDS (2.1 equiv.), dry THF, -78°C ; ii-1,2- $^{13}\text{C}_2$ -ethyl acetate (1 equiv.), -78°C , 15 min.; iii-1- ^{13}C -acetyl chloride (1.0 equiv.), -78°C , 30 min.; iv- ^1HCl 20 %; **b)** K_2CO_3 (1.1 equiv.), $^{13}\text{C}^1\text{H}_3\text{-I}$ (1.1 equiv.), 0°C , 18h, EtO^1H ; **c)** Cs_2CO_3 (0.2 equiv.), $\text{P}(\text{OEt})_3$ (0.2 equiv.), O_2 , DMSO, 20h. **d)** i- NaO^2H (2.5M), $^2\text{H}_2\text{O}$; ii- ^2HCl 35%; Tris buffer pH 7.5; 27 % overall yield.



1
2 **Fig. 2** Assignment transfer from the backbone to Leu^{pro-S}, Val^{pro-S} and Ile-δ₁ methyl groups of
3 HSP90-NTD. Examples of 2D-extracts from 3D ‘out and back’ HCC (i), HC(C)C (a, d, f and j)
4 and HC(CC)C (b, e and g) experiments correlating ¹H (F₃) and ¹³C (F₂) methyl resonances with
5 ¹³C_β (blue) or ¹³C_α (red) in F₁ dimension. Panels c and h display the corresponding 2D HNCA
6 and HN(CA)CB extracts for Ile-81 (c) and Ile-151 (h) allowing to connect Leu-80-δ₂ (pro-S),
7 Ile-81-δ₁, Val-150-γ₂ (pro-S), Ile-151-δ₁ methyl groups to previously assigned backbone atoms.
8 3D spectra were recorded on an NMR spectrometer operating at a proton frequency of 600 MHz
9 using the U-[²H, ¹⁵N, ¹³C], Ile-[2, 3, 4, 4-²H₄; 1, 2, 3, 4-¹³C₄; [¹³C¹H₃]^{δ1}/[¹²C²H₃]^{γ2}], Leu-[2, 3,
10 3, 4-²H₄; 1, 2, 3, 4-¹³C₄; [¹³C¹H₃]^{pro-S}/[¹²C²H₃]^{pro-R}], Val-[2, 3-²H₂; 1, 2, 3-¹³C₃; [¹³C¹H₃]^{pro-}
11 ^S/[¹²C²H₃]^{pro-R}] labelled sample or U-[²H, ¹⁵N, ¹³C] labelled sample (3D HNCA and
12 HN(CA)CB). (k) and (l) represent magnetization transfer schemes correlating with the strips
13 (a, b, c, d, e) and (f, g, h, i, j), respectively. Except when specified, all hydrogen atoms are ²H.

1
2
3
4
5
6
7
8
9



10
11
12
13
14
15
16
17
18
19
20
21
22
23
24
25
26
27
28
29
30
31
32
33
34

Fig. 3 Assignment of HSP90-NTD methyl groups belonging to the flexible loop covering ATP binding site. The 2D SOFAST methyl TROSY spectra were recorded using either the isoleucine to valine mutant samples using U- ^2H , ^{12}C , ^{15}N]-Ile- $^{13}\text{C}^1\text{H}_3$ $^{\delta 1}$ labelling scheme, or the leucine to alanine mutant sample using U- ^2H , ^{12}C , ^{15}N]-Leu/Val- $^{13}\text{C}^1\text{H}_3$ $^{\text{pro-S}}$ labelling scheme. Spectra were recorded at 298 K on a NMR spectrometer operating at a proton frequency of 850 MHz. a) The HSP90-NTD mutant spectra of I104V. b) L107A. c) I110V. Each mutant spectrum extract (dark blue) was superimposed with the wild type protein extract (black).

1
2
3
4
5
6
7
8
9
10
11
12
13
14
15
16
17
18
19
20
21
22
23
24
25
26
27
28

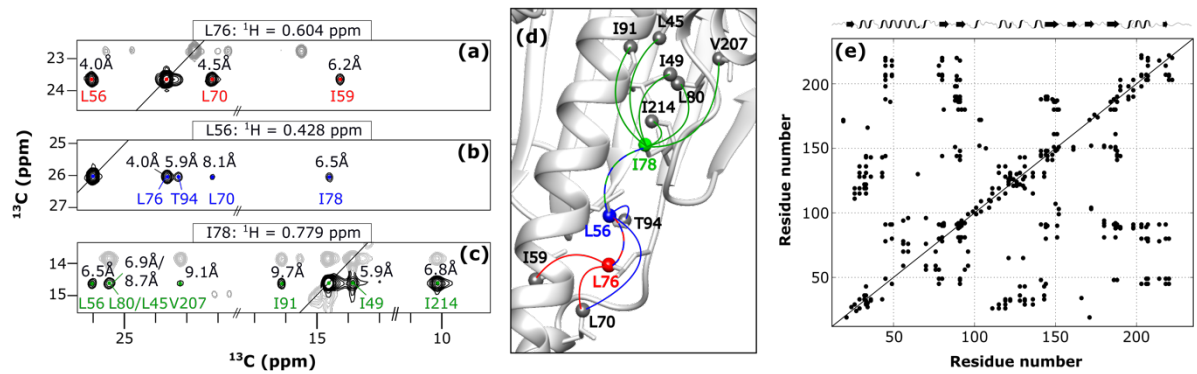
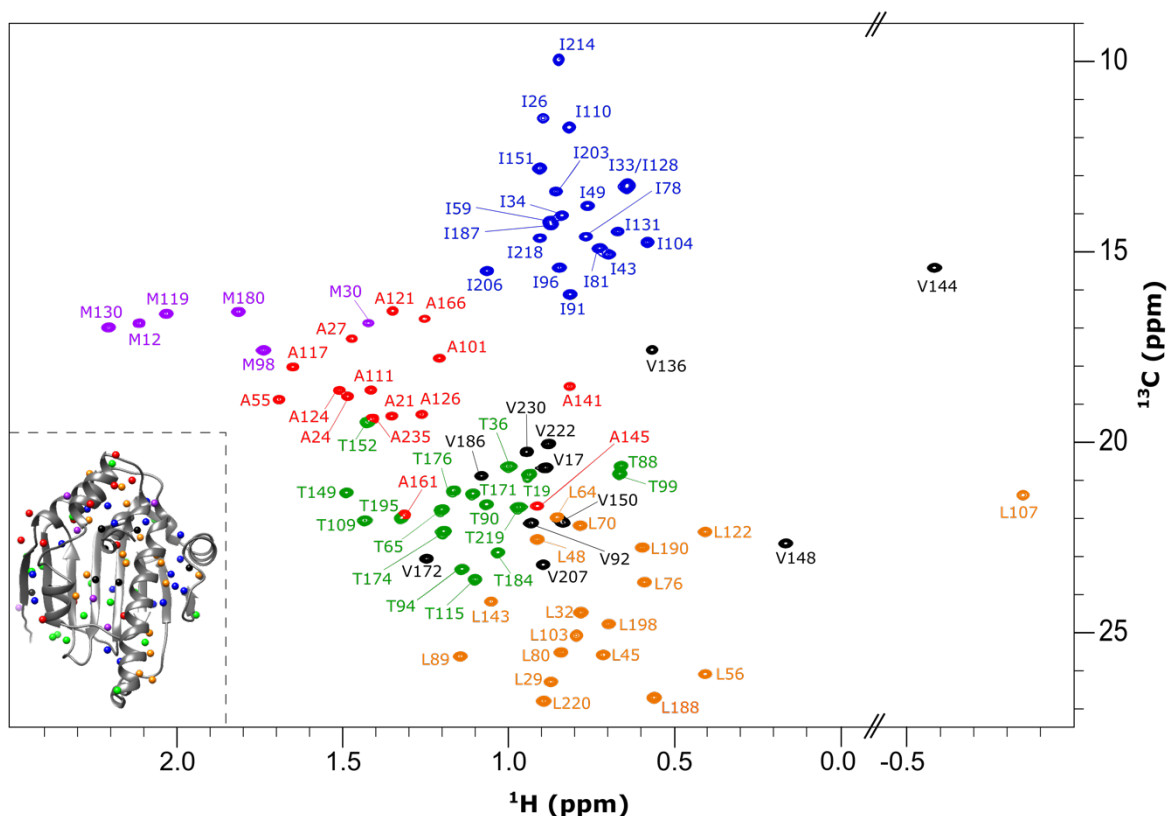


Fig. 4 Detected intermethyl NOEs in human HSP90-NTD. **a-c** Examples of 2D extracts of a 3D HMQC-NOESY-HMQC experiment recorded using U- ^{2}H , ^{12}C , ^{15}N -Leu/Val- $^{13}\text{C}^1\text{H}_3$ $^{\text{pro-S}}$, Ile- $^{13}\text{C}^1\text{H}_3$ $^{\delta 1}$, Met- $^{13}\text{C}^1\text{H}_3$ $^{\epsilon}$, Ala- $^{13}\text{C}^1\text{H}_3$ $^{\beta}$, Thr- $^{13}\text{C}^1\text{H}_3$ $^{\gamma}$ HSP90-NTD sample on a NMR spectrometer operating at a proton frequency of 950 MHz. The planes were extracted at the methyl proton frequencies of L76 (a), L56 (b) and I78 (c). The NOEs detected are colored in red, blue and green, respectively. **d** The NOEs detected in 2D extracts presented in panels a-c are displayed on the 3D structure of HSP90-NTD (PDB: 1YES) by lines (red for L76, blue for L56 and green for I78). **e** 2D matrix representing all the HSP90-NTD methyl residue pairs for which NOE cross-peaks have been detected.



1
2
3
4
5
6 **Fig. 5** Assigned 2D ^1H - ^{13}C SOFAST methyl TROSY spectrum of apo HSP90-NTD. Human
7 HSP90-NTD was perdeuterated and specifically $^{13}\text{C}^1\text{H}_3$ -labelled on Leu/Val- $^{13}\text{C}^1\text{H}_3$ ^{pro-S}, Ile-
8 $^{13}\text{C}^1\text{H}_3$ ^{δ1}, Met- $^{13}\text{C}^1\text{H}_3$ ^ε, Ala- $^{13}\text{C}^1\text{H}_3$ ^β, Thr- $^{13}\text{C}^1\text{H}_3$ ^γ methyl groups. Each signal is annotated
9 with the corresponding residue number. The spectrum was recorded on a NMR spectrometer
10 operating at a proton frequency of 950 MHz. On the bottom left side an insert represents the
11 3D structure of human HSP90-NTD (PDB: 1YES). The methyl groups are represented by
12 spheres. Alanines, isoleucines, valines, leucines, threonines and methionines are depicted in
13 red, dark blue, black, orange, light green and purple, respectively.

14
15
16
17
18
19
20

1 **Optimized Precursor to Simplify Assignment Transfer between Backbone**
2 **Resonances and Stereospecifically labelled Valine and Leucine Methyl**
3 **Groups: Application to Human Hsp90 N-Terminal Domain**

4
5
6 Faustine Henot¹, Rime Kerfah², Ricarda Törner¹, Pavel Macek^{1,2}, Elodie Crublet², Pierre
7 Gans¹, Matthias Frech³, Olivier Hamelin⁴, Jerome Boisbouvier¹. *

8
9
10 1. Univ. Grenoble Alpes, CNRS, CEA, Institut de Biologie Structurale (IBS),
11 71, avenue des martyrs, F-38044 Grenoble, France.

12 2. NMR-Bio, 5 place Robert Schuman, F-38025 Grenoble, France.

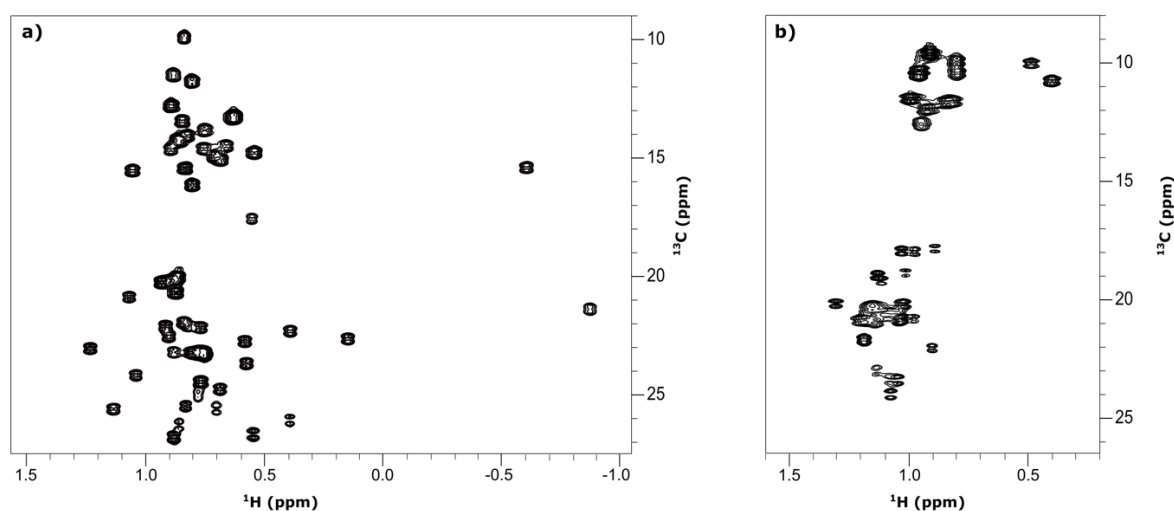
13 3. Discovery Technologies, Merck KGaA, Frankfurter Straße 250, 64293 Darmstadt, Germany.

14 4. Univ. Grenoble Alpes, CEA, CNRS, IRIG, CBM-F-38000 Grenoble. France.

15 * correspondence to be addressed to: jerome.boisbouvier@ibs.fr

16
17
18
19
20
21
22
23
24 **SUPPLEMENTARY INFORMATION**

1



2

3

4

5 **Fig. S1** 2D ^1H - ^{13}C SOFAST methyl TROSY spectrum of U- $[\text{}^2\text{H}$, ^{15}N , $^{13}\text{C}]$, Ile-[2, 3, 4, 4- $^2\text{H}_4$;
6 1, 2, 3, 4- $^{13}\text{C}_4$; $^{13}\text{C}^1\text{H}_3$] $^{\delta_1}$ / $[\text{}^{12}\text{C}^2\text{H}_3]^\gamma$], Leu-[2, 3, 3, 4- $^2\text{H}_4$; 1, 2, 3, 4- $^{13}\text{C}_4$; $[\text{}^{13}\text{C}^1\text{H}_3]^{\text{pro-S}}/[\text{}^{12}\text{C}^2\text{H}_3]^{\text{pro-}}$
7 R], Val-[2, 3- $^2\text{H}_2$; 1, 2, 3- $^{13}\text{C}_3$; $[\text{}^{13}\text{C}^1\text{H}_3]^{\text{pro-S}}/[\text{}^{12}\text{C}^2\text{H}_3]^{\text{pro-R}}$] HSP90-NTD **a)** and prefoldin **b)**
8 samples (labelling scheme A applied to prefoldin β subunit only), recorded before the HCC
9 experiments to check the sample quality. The labelling strategy used Ile- δ_1 precursor: sodium
10 (S)-2-hydroxy-2-(1',1'- $[\text{}^2\text{H}_2]$, 1', 2'- $[\text{}^{13}\text{C}_2]$) ethyl-3-oxo-1,2,3- $[\text{}^{13}\text{C}_3]$ -4,4,4- $[\text{}^2\text{H}_3]$ -butanoate)
11 and the suitably labelled acetolactate precursor: 1, 2, 3- $[\text{}^{13}\text{C}_3]$ -2- $[\text{}^{13}\text{C}^1\text{H}_3]$ -2- $[\text{O}^2\text{H}]$ -3-oxo-4, 4,
12 4- $[\text{}^2\text{H}_3]$ -butanoate for the labelling of Leu and valine pro-S methyl groups. No additional peaks
13 were detected neither to the pro-R methyls groups of leucine and valine nor to the isoleucine-
14 γ_2 site, confirming the absence of isotopic scrambling. The peaks are splitted in the carbon
15 dimension due to the presence of $^1J_{\text{CC}}$ coupling as expected from the labelling scheme of the
16 produced samples.

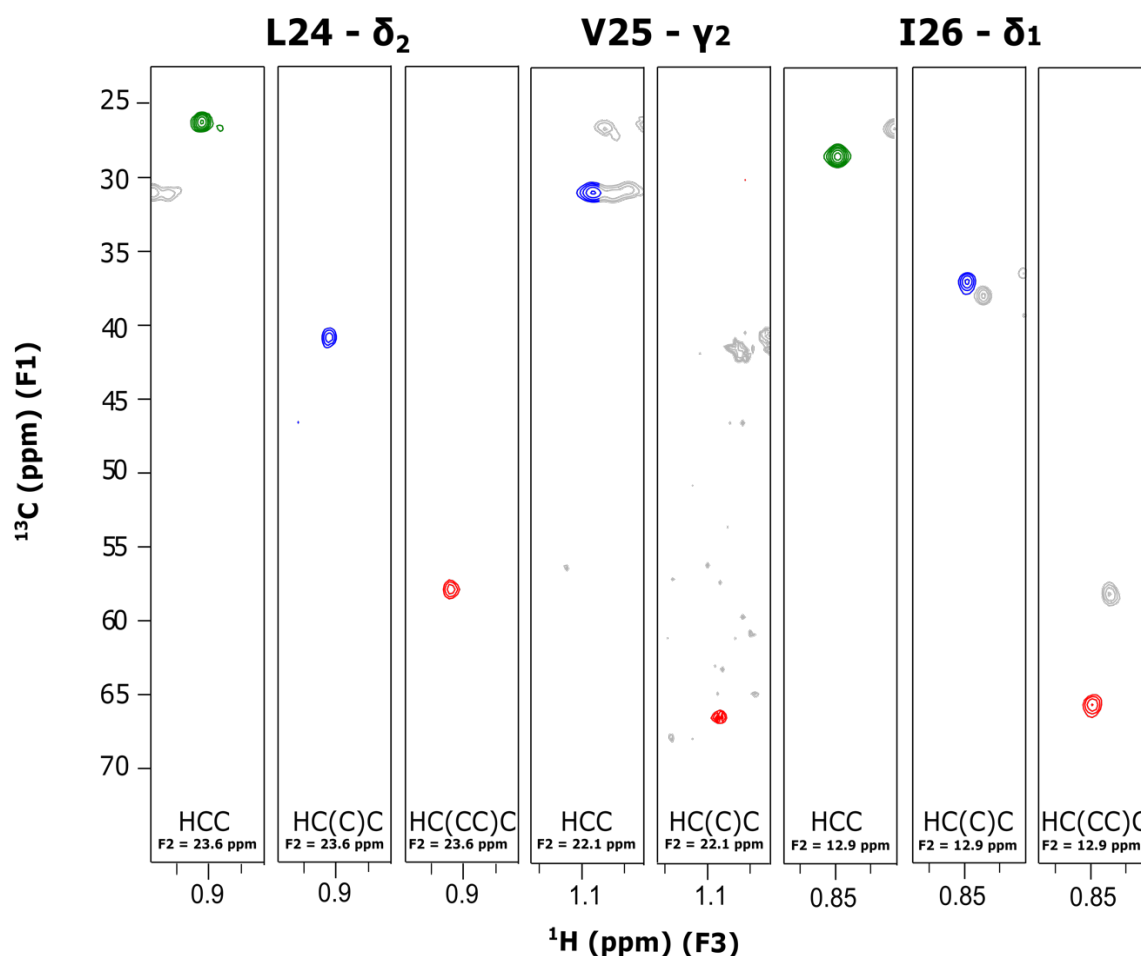
17

18

19

20

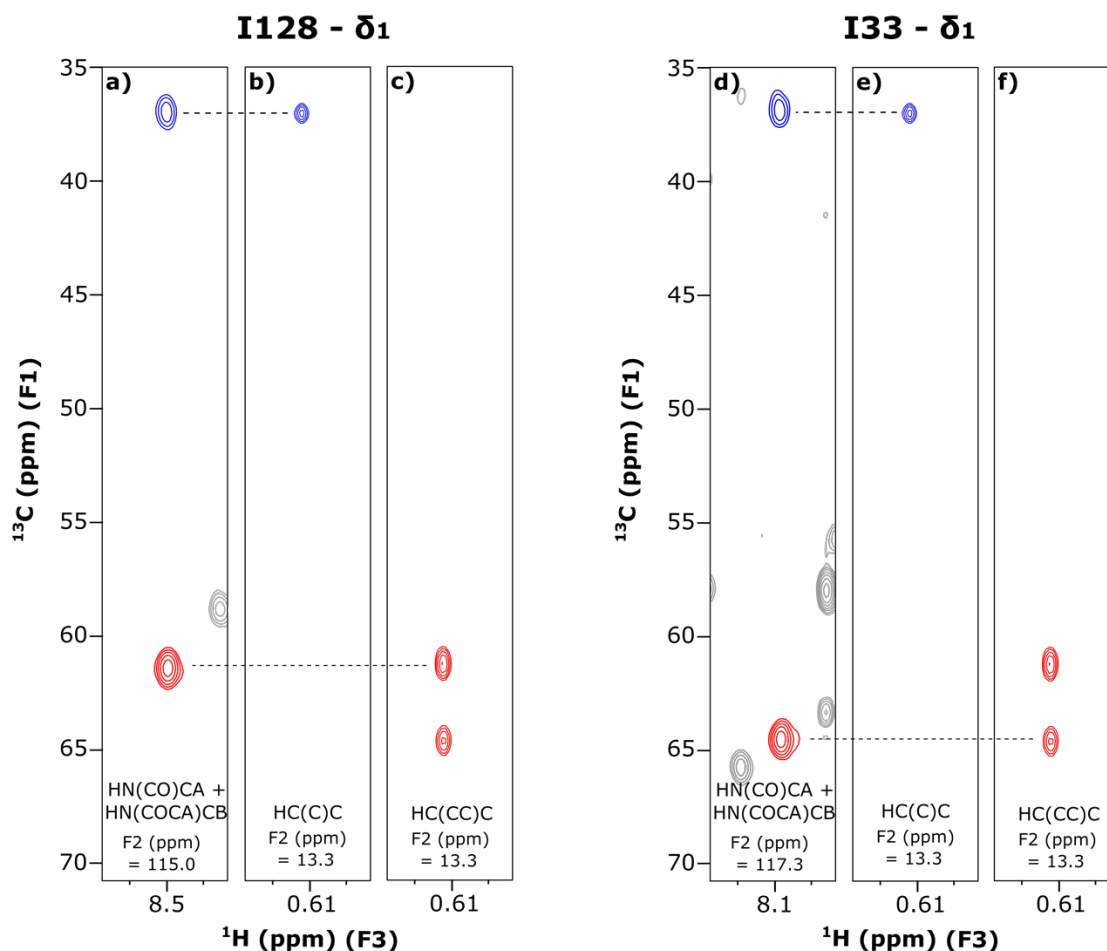
21



1
2
3 **Fig. S2** Application to the 87 kDa prefoldin from *Pyrococcus horikoshii*. Examples of 2D-
4 extracts from 3D ‘out and back’ HCC , HC(C)C and HC(CC)C experiments correlating ^1H (F₃)
5 and ^{13}C (F₂) methyl resonances with $^{13}\text{C}_\gamma$ (green) $^{13}\text{C}_\beta$ (blue) or $^{13}\text{C}_\alpha$ (red) in F₁ dimension of
6 Leu-24, Val-25 and Ile-26 of *Pyrococcus horikoshii* prefoldin subunit β . Spectra have been
7 recorded at 310 K using 0.2 mM U- ^{2}H , ^{15}N , ^{13}C], Ile-[2, 3, 4, 4- $^2\text{H}_4$; 1, 2, 3, 4- $^{13}\text{C}_4$;
8 $^{13}\text{C}^1\text{H}_3$] $^{\delta 1}$ /[$^{12}\text{C}^2\text{H}_3$] $^{\gamma 2}$], Leu-[2, 3, 3, 4- $^2\text{H}_4$; 1, 2, 3, 4- $^{13}\text{C}_4$; [$^{13}\text{C}^1\text{H}_3$] $^{\text{pro-S}}$ /[$^{12}\text{C}^2\text{H}_3$] $^{\text{pro-R}}$], Val-[2, 3-
9 $^2\text{H}_2$; 1, 2, 3- $^{13}\text{C}_3$; [$^{13}\text{C}^1\text{H}_3$] $^{\text{pro-S}}$ /[$^{12}\text{C}^2\text{H}_3$] $^{\text{pro-R}}$] sample of prefoldin on an NMR spectrometer
10 operating at a proton frequency of 950 MHz. The acquisition parameters were similar to that
11 used for HSP90-NTD, described in Materials and Methods section. Prefoldin was expressed
12 and purified according to the protocol described in Törner et al. (2020) and labelled on the β
13 subunit only using labelling scheme A, described in Materials and Methods section of the
14 present manuscript.

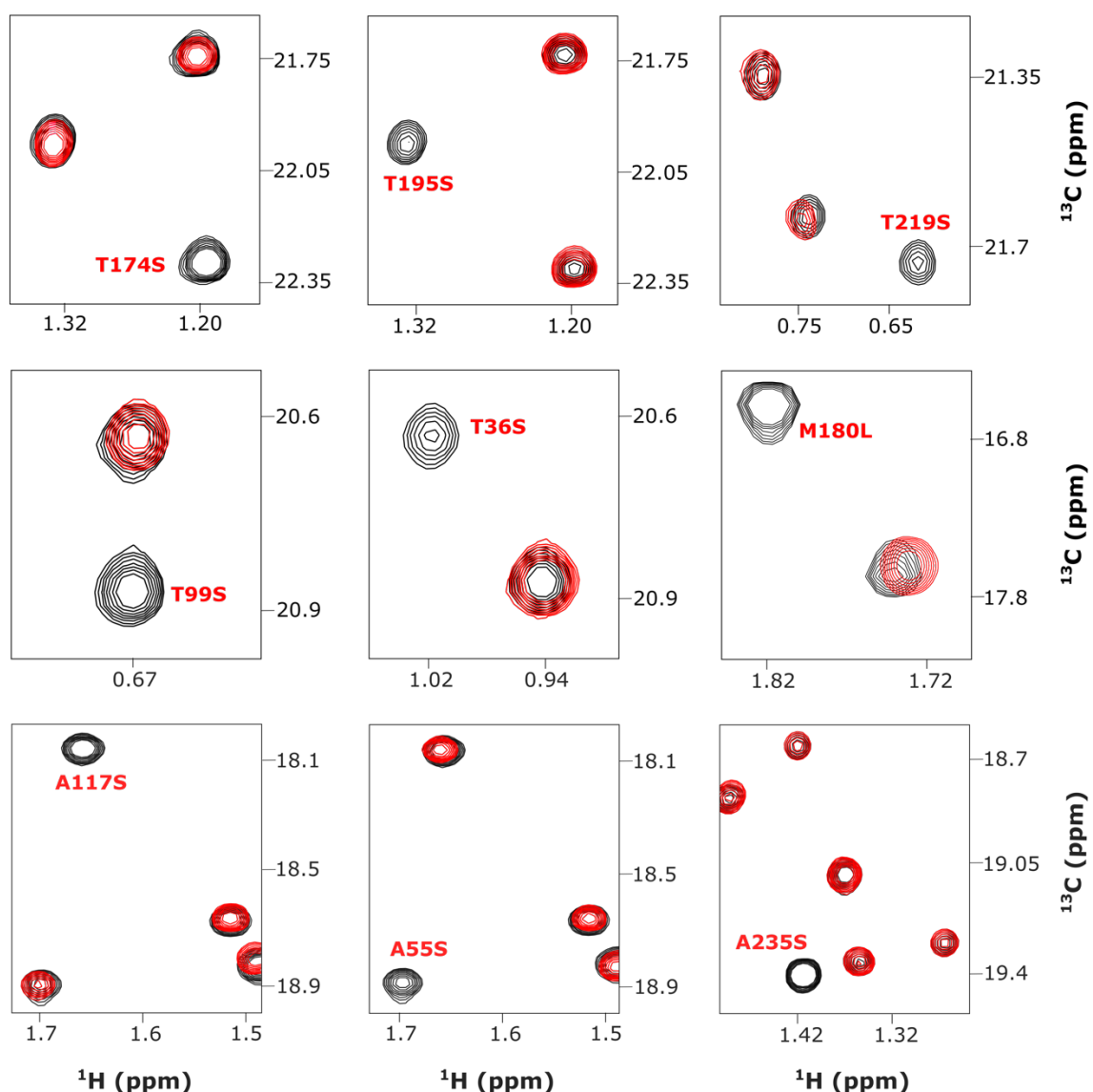
15
16
17
18

1
2



3
4
5
6

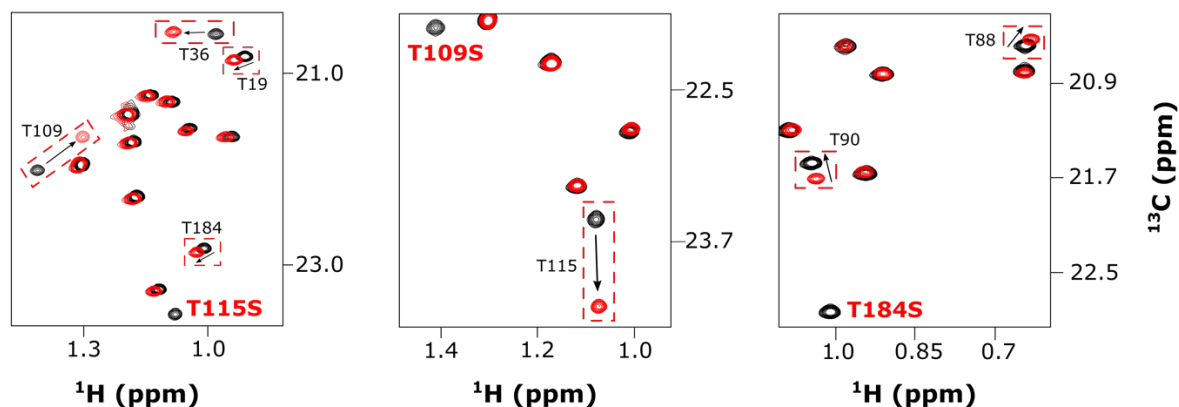
7 **Fig. S3** Assignment transfer from the backbone to the Ile- δ_1 methyl groups of Ile-33 and Ile-
8 128 of HSP90-NTD. Examples of 2D-extracts from 3D ‘out and back’ HC(C)C (b and e) and
9 HC(CC)C (c and f) experiments correlating ^1H (F₃) and ^{13}C (F₂) methyl resonances with $^{13}\text{C}_\beta$
10 (blue) or $^{13}\text{C}_\alpha$ (red) in F₁ dimension. Panels a and d display the corresponding 2D HN(CO)CA
11 and HN(COCA)CB extracts for Ile-128 (a) and Ile-33 (d) allowing to connect Ile-33- δ_1 and Ile-
12 128- δ_1 methyl groups to previously assigned backbone atoms. 3D spectra were recorded on an
13 NMR spectrometer operating at a proton frequency of 600 MHz using the U- ^{2}H , ^{15}N , ^{13}C , Ile-
14 [2, 3, 4, 4- $^2\text{H}_4$; 1, 2, 3, 4- $^{13}\text{C}_4$; $^{13}\text{C}^1\text{H}_3$] $^{\delta_1}$ /[$^{12}\text{C}^2\text{H}_3$] $^{\gamma_2}$, Leu-[2, 3, 3, 4- $^2\text{H}_4$; 1, 2, 3, 4- $^{13}\text{C}_4$;
15 [$^{13}\text{C}^1\text{H}_3$] $^{\text{pro-S}}$ /[$^{12}\text{C}^2\text{H}_3$] $^{\text{pro-R}}$], Val-[2, 3- $^2\text{H}_2$; 1, 2, 3- $^{13}\text{C}_3$; [$^{13}\text{C}^1\text{H}_3$] $^{\text{pro-S}}$ /[$^{12}\text{C}^2\text{H}_3$] $^{\text{pro-R}}$] labelled
16 sample or U- ^{2}H , ^{15}N , ^{13}C labelled sample (3D HN(CO)CA and HN(COCA)CB).



1
2
3
4 **Fig. S4** Assignment of methyl groups using mutagenesis. Examples of 2D ^1H - ^{13}C SOFAST
5 methyl TROSY spectra of HSP90-NTD mutants, for which no or minor chemical shift
6 perturbations are observed. Spectra were acquired on an NMR spectrometer operating at a
7 proton frequency of 850 MHz. Each mutant spectrum extract (colored) is superimposed with
8 the corresponding spectra acquired using wild type HSP90-NTD methyl labelled spectra
9 (black). The signal corresponding to each mutant is annotated in color. List of the mutants
10 produced for this study: M12L, M30L M119L, M130L, M180L, A21S, A24S, A27S, A55S,
11 A101S, A111S, A117S, A121S, A124S, A126S, A161S, A166S, A235S, T19S, T36S, T65S,
12 T99S, T109S, T115S, T152S, T171S, T174S, T184S, T195S, T219S, I104V, L107A, I110V.

13
14

1
2



3
4
5
6
7
8
9
10
11
12
13
14
15
16
17
18
19
20
21
22

Fig. S5 Assignment of methyl groups using mutagenesis. Examples of 2D ^1H - ^{13}C SOFAST methyl TROSY spectra of HSP90-NTD mutants, for which chemical shift perturbations. Spectra were acquired on an NMR spectrometer operating at a proton frequency of 850 MHz. Each mutant spectrum extract (colored) is superimposed with the corresponding spectra acquired using wild type HSP90-NTD methyl labelled spectra (black). The signal corresponding to each mutant is annotated in color. Black arrows represent secondary chemical shifts.

Table S1: Output file from MAGIC software for the assignment of HSP90-NTD methyl groups.

The 1st column displays the best assignment. The 2nd and 3rd columns give the ¹³C and ¹H chemical shifts, respectively. The 4th column represents the sum of all peak-peak connection confident scores for each peak. The 5th column shows the NOE assignment completeness of the strip related to each peak and the 6th column displays the list of all possible assignment with their scores (Monneau et al. 2017).

The automated methyl assignment was performed using the reference structure of HSP90-NTD (PDB: 1YES). MAGIC was run with a score threshold factor of 1, distance thresholds of 7–10 Å and using the 344 inter methyl NOE cross peaks (S/N ≥ 5) detected (Fig. 4e). In addition, MAGIC was given the methyl type for each methyl group, previously identified using specific methyl labelling. In blue are the methyl groups assigned automatically by MAGIC that have 1) a single assignment, 2) a high NOE assignment completeness of the strip related to each peak (> 50 %) and 3) a high total confidence score value (≥ 7).

Predicted Assignment	¹³ C ppm	¹ H ppm	Score	% NOE	Possible Assignment
V144CG*-HG*	15.487	-0.566	31.48	0.86	{'V144CG': 215.504}
L56CD*-HD*	26.036	0.428	9.0	1.0	{'L56CD': 215.504}
L89CD*-HD*	25.59	1.159	26.22	1.0	{'L89CD': 215.504}
L45CD*-HD*	25.544	0.731	36.08	1.0	{'L80CD': 207.896 'L45CD': 215.504}
L80CD*-HD*	25.474	0.86	33.17	1.0	{'L80CD': 215.504 'L45CD': 207.896}
L198CD*-HD*	24.747	0.717	15.0	1.0	{'L198CD': 215.504}
L32CD*-HD*	24.451	0.802	13.67	0.8	{'L32CD': 215.504}
L143CD*-HD*	24.158	1.061	13.0	1.0	{'L143CD': 215.504 'L122CD': 206.867}
L76CD*-HD*	23.647	0.605	9.0	1.0	{'L70CD': 207.413 'L76CD': 215.504}
T94CG2-HG2	23.292	1.157	7.0	1.0	{'T184CG2': 206.767 'T152CG2': 207.402 'T94CG2': 215.504}
T115CG2-HG2	23.566	1.118	24.6	1.0	{'T115CG2': 215.504}
M130CE-HE	17.026	2.213	5.0	0.25	{'M130CE': 215.504}
V207CG*-HG*	23.223	0.91	27.69	1.0	{'V207CG': 215.504}
V172CG*-HG*	23.024	1.257	3.0	0.5	{'V172CG': 215.504}
L190CD*-HD*	22.76	0.615	33.53	1.0	{'L190CD': 215.504}
V148CG*-HG*	22.646	0.178	24.0	0.83	{'V148CG': 215.504}
L48CD*-HD*	22.527	0.93	19.5	0.67	{'L48CD': 215.504}
T19CG2-HG2	22.331	1.204	2.0	0.0	{'T19CG2': 215.504 'T176CG2': 215.504 'T174CG2': 215.504 'T171CG2': 215.504}
V92CG*-HG*	22.125	0.946	27.35	1.0	{'V92CG': 215.504}
L70CD*-HD*	22.186	0.801	10.39	1.0	{'L70CD': 215.504 'L76CD': 207.413}
I214CD1-HD1	10.135	0.86	13.38	1.0	{'I78CD1': 207.021 'I214CD1': 215.504}
I26CD1-HD1	11.564	0.908	14.0	1.0	{'I26CD1': 215.504}
I110CD1-HD1	11.885	0.831	2.0	1.0	{'I110CD1': 215.504}
I151CD1-HD1	12.894	0.916	15.0	0.57	{'I151CD1': 215.504}
I33CD1-HD1	13.355	0.661	36.6	1.0	{'I33CD1': 215.504}
I203CD1-HD1	13.467	0.874	33.35	1.0	{'I203CD1': 215.504}
I49CD1-HD1	13.848	0.775	34.45	0.86	{'I49CD1': 215.504}

I34CD1-HD1	14.091	0.859	2.0	1.0	{'I34CD1': 215.504}	
I187CD1-HD1	14.32	0.88	12.37	1.0	{'I187CD1': 215.504}	
I59CD1-HD1	14.25	0.89	8.37	0.75	{'I96CD1': 207.538}	'I59CD1': 215.504}
I131CD1-HD1	14.458	0.688	23.0	0.86	{'I131CD1': 215.504}	
I78CD1-HD1	14.622	0.779	24.0	1.0	{'I218CD1': 207.374 'I214CD1': 207.021}	'I78CD1': 215.504
M119CE-HE	16.667	2.047	26.67	0.71	{'M119CE': 215.504}	
I218CD1-HD1	14.66	0.916	22.0	0.8	{'I218CD1': 215.504 'I214CD1': 206.692}	'I78CD1': 207.374
I104CD1-HD1	14.808	0.565	4.0	1.0	{'I104CD1': 215.504}	
I81CD1-HD1	14.949	0.733	42.89	0.45	{'I81CD1': 215.504}	
I43CD1-HD1	15.1	0.714	10.0	1.0	{'I43CD1': 215.504}	'I128CD1': 208.077}
I96CD1-HD1	15.467	0.865	5.92	0.67	{'I96CD1': 215.504}	'I59CD1': 207.538}
I206CD1-HD1	15.535	1.076	28.33	0.83	{'I206CD1': 215.504}	
I91CD1-HD1	16.128	0.832	77.51	0.81	{'I91CD1': 215.504}	
A124CB-HB	16.617	1.357	6.0	0.67	{'A121CB': 215.504 'A124CB': 215.504}	'A126CB': 207.223
A166CB-HB	16.771	1.262	2.0	1.0	{'A166CB': 215.504}	
A27CB-HB	17.326	1.486	2.0	1.0	{'A27CB': 215.504}	'A24CB': 215.504}
V136CG*-HG*	17.675	0.576	19.67	1.0	{'V136CG': 215.504}	
A101CB-HB	17.824	1.225	3.0	1.0	{'A101CB': 215.504}	
A141CB-HB	18.538	0.827	15.0	1.0	{'A145CB': 207.062}	'A141CB': 215.504}
A121CB-HB	18.655	1.528	4.33	1.0	{'A121CB': 215.504 'A126CB': 207.223}	'A117CB': 207.058 'A124CB': 215.504}
A111CB-HB	18.69	1.429	5.0	1.0	{'A111CB': 215.504 'A24CB': 207.059}	'A27CB': 207.455
A24CB-HB	18.812	1.5	2.0	1.0	{'A27CB': 215.504}	'A24CB': 215.504}
A126CB-HB	19.272	1.272	9.83	1.0	{'A121CB': 207.223}	'A126CB': 215.504}
M180CE-HE	16.604	1.829	29.55	0.64	{'M180CE': 215.504}	
T152CG2-HG2	19.402	1.427	3.23	0.4	{'T152CG2': 215.504}	
V222CG*-HG*	20.053	0.894	5.0	1.0	{'V222CG': 215.504}	
T36CG2-HG2	20.646	1.008	8.0	1.0	{'T36CG2': 215.504}	
T88CG2-HG2	20.629	0.675	8.0	0.75	{'T88CG2': 215.504}	'T195CG2': 207.358}
T99CG2-HG2	20.83	0.676	2.0	0.33	{'T99CG2': 215.504}	
L220CD*-HD*	26.75	0.906	12.31	1.0	{'L220CD': 215.504}	
V186CG*-HG*	20.862	1.1	19.26	0.57	{'V150CG': 207.024}	'V186CG': 215.504}
T176CG2-HG2	21.263	1.172	2.0	0.0	{'T171CG2': 215.504 'T174CG2': 215.504}	'T176CG2': 215.504 'T19CG2': 215.504}
T149CG2-HG2	21.331	1.498	9.0	1.0	{'T149CG2': 215.504}	
A145CB-HB	21.67	0.932	16.27	1.0	{'A145CB': 215.504}	'A141CB': 207.062}
T90CG2-HG2	21.638	1.078	29.0	0.71	{'T90CG2': 215.504}	
T195CG2-HG2	21.988	1.34	5.0	1.0	{'T195CG2': 215.504}	'T88CG2': 207.358}
L188CD*-HD*	26.645	0.575	38.1	0.78	{'L188CD': 215.504}	
T109CG2-HG2	22.02	1.444	3.0	1.0	{'T109CG2': 215.504}	
L122CD*-HD*	22.419	0.431	8.1	0.75	{'L143CD': 206.867}	'L122CD': 215.504}
L103CD*-HD*	24.974	0.797	2.73	1.0	{'L103CD': 215.504 'L64CD': 207.687}	'L107CD': 207.733
A161CB-HB	21.9	1.327	7.0	0.67	{'A161CB': 215.504}	

L29CD*-HD*	26.252	0.89	27.0	1.0	{'L29CD': 215.504}
A55CB-HB	19.402	1.427	3.23	0.0	{'A24CB': 208.147 'A166CB': 208.147 'A21CB': 215.504 'A111CB': 207.455 'A27CB': 208.147 'A117CB': 215.504 'A235CB': 215.504 'A55CB': 215.504 'A124CB': 207.058}
T65CG2-HG2	20.867	0.944	2.0	0.0	{'T171CG2': 215.504 'T176CG2': 215.504 'T174CG2': 215.504 'T65CG2': 215.504 'T19CG2': 215.504 'T219CG2': 215.504}
T184CG2-HG2	21.357	1.117	2.0	1.0	{'T171CG2': 207.047 'T152CG2': 207.267 'T94CG2': 206.547 'T176CG2': 207.047 'T174CG2': 207.047 'T65CG2': 207.047 'T19CG2': 207.047 'T219CG2': 207.047 'T184CG2': 215.504}
T219CG2-HG2	21.756	1.216	3.0	0.0	{'T171CG2': 215.504 'T152CG2': 208.147 'T94CG2': 207.402 'T176CG2': 215.504 'T174CG2': 215.504 'T65CG2': 215.504 'T19CG2': 215.504 'T219CG2': 215.504 'T184CG2': 207.267}

1
2

Not Assigned	¹³ C ppm	¹ H ppm	
3	16.949	2.087	NotAss ['M30CE' 'M98CE' 'M12CE']
5	17.58	1.732	NotAss ['M30CE' 'M98CE' 'M12CE']
49	16.898	1.43	NotAss ['M30CE' 'M98CE' 'M12CE']
53	18.034	1.659	NotAss ['A21CB' 'A117CB' 'A235CB']
58	18.938	1.694	NotAss ['A21CB' 'A117CB' 'A235CB']
60	19.325	1.362	NotAss ['A21CB' 'A117CB' 'A235CB']
64	20.266	0.959	NotAss ['V17CG' 'V150CG' 'V230CG']
67	20.699	0.9	NotAss ['V17CG' 'V150CG' 'V230CG']
73	21.392	-0.838	NotAss ['L64CD' 'L107CD']
75	21.709	0.974	NotAss ['T171CG2' 'T174CG2']
80	21.965	0.865	NotAss ['L64CD' 'L107CD']
82	22.208	0.844	NotAss ['V17CG' 'V150CG' 'V230CG']
86	22.86	1.022	NotAss ['T171CG2' 'T174CG2']

3

1 **Table S2: Assignment of HSP90-NTD methyl groups**

2
3

Met	H(ϵ)	C(ϵ)
M12	2.117	16.889
M30	1.426	16.886
M98	1.741	17.594
M119	2.035	16.644
M130	2.210	17.000
M180	1.818	16.593

4

Thr	H(γ_2)	C(γ_2)
T19	0.942	20.832
T36	1.002	20.622
T65	1.205	21.746
T88	0.664	20.605
T90	1.07	21.611
T94	1.144	23.293
T99	0.667	20.819
T109	1.437	22.033
T115	1.104	23.567
T149	1.492	21.304
T152	1.430	19.470
T171	1.111	21.333
T174	1.199	22.314
T176	1.169	21.250
T184	1.036	22.863
T195	1.326	21.960
T219	0.973	21.686

5

Ala	H(β)	C(β)
A21	1.356	19.310
A24	1.489	18.799
A27	1.476	17.297
A55	1.696	18.870
A101	1.211	17.806
A111	1.419	18.635
A117	1.654	18.031
A121	1.353	16.570
A124	1.514	18.640
A126	1.265	19.266
A141	0.819	18.528
A145	0.917	21.654
A161	1.318	21.910
A166	1.257	16.777
A235	1.415	19.384

6

Ile	H(δ_1)	C(δ_1)
I26 ^b	0.899	11.547
I33/I128 ^a	0.647	13.317
I34 ^a	0.842	14.078
I43 ^a	0.702	15.097
I49 ^a	0.765	13.830
I59 ^a	0.876	14.287
I78 ^a	0.771	14.631
I81 ^a	0.729	14.935
I91 ^a	0.818	16.139
I96 ^a	0.850	15.440
I104 ^a	0.585	14.778
I110 ^b	0.821	11.783
I131 ^a	0.675	14.498
I151 ^a	0.910	12.853
I187 ^a	0.876	14.287
I203 ^a	0.861	13.455
I206 ^a	1.069	15.528
I214 ^a	0.853	10.015
I218 ^a	0.909	14.670

1

Leu	H(δ_2)	C(δ_2)
L29 ^c	0.876	26.240
L32 ^c	0.786	24.429
L45 ^d	0.719	25.537
L48 ^c	0.918	22.526
L56 ^c	0.411	26.037
L64 ^c	0.853	21.951
L70 ^c	0.787	22.168
L76 ^c	0.594	23.642
L80 ^c	0.846	25.472
L89 ^c	1.149	25.579
L103 ^c	0.798	25.037
L107 ^d	-0.851	21.374
L122 ^c	0.411	22.329
L143 ^d	1.056	24.148
L188 ^d	0.565	26.652
L190 ^c	0.601	22.739
L198 ^c	0.702	24.73
L220 ^c	0.898	26.742

2

Val	H(γ_2)	C(γ_2)
V17 ^d	0.892	20.658
V92 ^c	0.936	22.102
V136 ^c	0.570	17.586
V144 ^c	-0.582	15.446

V148 ^c	0.168	22.630
V150 ^c	0.839	22.084
V172 ^c	1.251	23.028
V186 ^c	1.085	20.870
V207 ^c	0.899	23.183
V222 ^c	0.884	20.037
V230	0.949	20.244

1

2

3

4 ^a Residues assigned by (Park et al. 2011) and confirmed by this study.

5 ^b Assignment was inverted for these two residues in our study compared to (Park et al. 2011).

6 ^c Residues stereospecifically assigned by (Lescanne et al. 2018) and confirmed by this study.

7 ^d Stereospecific assignment was inverted compared to (Lescanne et al. 2018).